Spatial organisation of Listeria monocytogenes and Escherichia coli O157:H7 cultivated in gel matrices

Cédric Saint Martin, Maud Darsonval, Marina Grégoire, Nelly Caccia, Lucas Midoux, Sophie Berland, Sabine Leroy, Florence Dubois-Brissonnet, Mickaël Desvaux, Romain Briandet

Spatial organisation of *Listeria monocytogenes* and *Escherichia coli* O157:H7 cultivated in gelled matrices

Cédric SAINT MARTIN[1,2], Maud DARSONVAL[1], Marina GRÉGOIRE[1], Nelly CACCIA[2], Lucas MIDOUX[1], Sophie BERLAND[3], Sabine LEROY[2], Florence DUBOIS-BRISSONNET[1], Mickaël DESVAUX[2]* & Romain BRIANDET[1]*

[1] Université Paris-Saclay, INRAE, AgroParisTech, MICALIS Institute, 78350 Jouy-en-Josas France,
[2] Université Clermont Auvergne, INRAE, UMR454 MEDIS, 63000 Clermont-Ferrand, France,
[3] Université Paris-Saclay, INRAE, AgroParisTech, SayFood, 91300 Massy, France.

*Corresponding authors: M. Desvaux (mickael.desvaux@inrae.fr) & R. Briandet (romain.briandet@inrae.fr)

Abstract

Spatial organisation of bacterial pathogens in food matrices remains poorly understood but of importance to improve risk assessment and prevent infection of consumers by contaminated foodstuff. Combining confocal laser scanning microscopy with genetic fluorescent labelling of key foodborne bacterial pathogens *Listeria monocytogenes* and *Escherichia coli* O157:H7 permitted to investigate the spatial patterns of colonisation of both pathogens in gel matrices, alone or in combination, in various environmental conditions. Increasing low melting point agarose (LMPA) concentrations triggers the transition between motile single cell lifestyle to a sessile population spatially organised as microcolonies. The size, number and morphology of microcolonies were highly affected by supplementations in NaCl or lactic acid, two compounds frequently used in food products. Strikingly, single-cell motility was partially restored at higher LMPA concentration in presence of lactic acid for *E. coli* O157:H7 and in presence of NaCl for *L. monocytogenes*. Co-culture of both species in the hydrogel affected pathogen colonisation features. *L. monocytogenes* presented a better ability to colonise gel matrices containing lactic acid in presence of *E. coli* O157:H7. Altogether, this investigation provides advanced insights in spatial distribution and structural dynamics of bacterial pathogens in gel matrices. Potential impacts on food safety are further discussed.

Keywords

L. monocytogenes, E. coli O157:H7, food matrix, hydrogel, spatial organisation, Confocal Laser Scanning Microscopy (CLSM)

Abbreviations

CLSM stands for "Confocal Laser Scanning Microscopy"

LMPA stands for "Low Melting Point Agarose"

1) Introduction

In Europe, *Listeria monocytogenes* and *Escherichia coli* O157:H7 ranked as the third and fifth most common foodborne zoonotic agents, respectively, with a number of related cases on the slow rise for over 8 years (EFSA and ECDC; 2021). *E. coli* O157:H7 is generally associated with meat contamination because of its presence in the digestive tract of livestock, but contamination of other products such as raw-milk products or vegetables has been recently reported (Luna-Guevara et al., 2019). As a food contaminant, *L. monocytogenes* is mostly found in vegetables, fish and cheese, but being a saprophyte and ubiquitous microorganism, the panel of possible vectors is quite wide including soil, water or animals (Kallipolitis et al., 2020). Detection and control of bacterial load in food matrix is hindered by the fact that current predictive models are derived from planktonic bacterial growth that proved to be poorly accurate when applied to bacterial growth in solid and semi-solid food matrices (Pin et al., 1999; Skandamis and Jeanson, 2015; Smith and Schaffner, 2004). Actually, food matrices are spatially organised environment with heterogeneous microstructures harbouring multiple micro-gradients that evolve with time and microbial activity, *e.g.* oxygen concentration, pH, temperature, nutrients consumption or metabolite accumulation (Lobete et al., 2015). There is no generic model yet to describe substrates diffusion limitations effects in such food matrices and the one existing can be contradictory (Cussler, 1997; Ribeiro et al., 2005). As a general rule, small molecules with less reactivity to the matrix (neutral charge or same charge as the reticulating agent) will diffuse faster, and large polymers with flexible chains diffuse more easily than rigid molecules of the same radius (Silva et al., 2013). Local heterogeneities and their dynamics can lead to differentiation in microbial populations as cells can undergo

adaptive responses to a given environment such as genotypic variation and stochastic gene expression (Stewart and Franklin, 2008). This heterogeneity of expression can lead to phenotypic diversity of cell subpopulations, expanding the possibilities of multiple stress tolerance or virulence levels for a same species in the same environment (Caniça et al., 2019; Nielsen et al., 2013). The repartition and physiology of bacterial cells in a food matrix is also dependent on the texture of the media. Matrix hardness alters bacterial motility both on surfaces and inside the matrix itself (Yang et al., 2017). The decrease in speed is also coupled with the selection of swimming behaviour between “runs" and “tumbles” as meshes of reticulating agents create traps that limit diffusion through straight trajectories (Licata et al., 2016). Studies on the growth of bacteria inside gelled nutritive matrix are still sparse. Most of those concern predictive modelling and population survival under stress exposure (Antwi et al., 2006; Costello et al., 2018; Jeanson et al., 2015; Kabanova et al., 2012). While the behaviour of cheese starters such as *Lactococcus lactis* has been described (Theys et al., 2009, 2008), only a few investigations have been dedicated to pathogens such as *Listeria monocytogenes* (Uyttendaele et al., 2009; Verheyen et al., 2019) and, to our knowledge, none to *E. coli* O157:H7. In order to explore the behaviour of foodborne pathogens in semi-solid food matrices, *L. monocytogenes* and *E. coli* O157:H7 were grown in synthetic gelled media mimicking relevant food matrices such as grounded meat or soft cheese. Using fluorescent bacterial strains, spatial organisation and dynamics of the pathogens was investigated *in situ* by confocal laser scanning microscopy (CLSM). This experimental setup allowed the extraction and analysis of the microcolonies size and morphological parameters as well as single-cell motility in various environmental conditions. The gelled matrix was tuned with different concentrations of low melting point agarose (LMPA) to change the hydrogel texture and to study the variation of cell motility and spatially organised sessile microcolonies. Besides, different NaCl and lactic acid concentrations were considered respective to conditions encountered by these pathogens in food.

2) Materials and methods

Bacterial strains and culture conditions

From cryotubes conserved at -80°C, bacterial strains were plated on Petri dishes with TSB (Tryptone Soya Broth, Oxoid, reference CM0129) agar and incubated overnight at 37°C. One

bacterial colony was picked up and inoculated in TSB broth prior to overnight incubation under orbital shaking. When required, growth media were supplemented either with tetracycline (10 µg.mL^{-1}; ALFA AESAR, reference B21408) or chloramphenicol (25 µg.mL^{-1}; EUROMEDEX, reference 3886-B). *L. monocytogenes* EGDe (Glaser et al., 2001) was transformed by electroporation with the plasmid pNF8 constitutively expressing the green fluorescent protein GFPmut2 (Cormack et al., 1996; Fortineau et al., 2000). Non-cytotoxic *E. coli* O157:H7 CM454 (Gobert et al., 2007; Renier et al., 2014) was transformed with the plasmid pVaAg-Red constitutively expressing the red fluorescent protein mRuby2 (Ageorges et al., 2019).

Gelled matrices

To mimic semi-solid food matrices, such as minced meat and soft cheese, gelled matrices of different textures were obtained using low melting point agarose (LMPA; UltraPure Agarose, Invitrogen, reference 16500-500) at various concentrations (*i.e.* 0.25 %, 0.50 % and 1.00 %). From overnight pre-cultures and following serial dilutions, the bacterial inoculum was adjusted to attain the desired initial concentration. After boiling to ensure complete melting, the TSB-LMPA was kept at 60°C and cooled down below 40°C just before adding the bacterial inoculum to prevent heat stress. Medium could be supplemented with lactic acid (Sigma Aldrich, 27715-1L-R) to ajust media to pH5 (8 10^{-4}mM) and/or 25 g/L NaCl (AnalaR NORMAPUR, VWR chemicals 27810.295). After homogenising and gentle stirring to avoid bubble formation, the inoculated gel matrix was immediately distributed in each well of a 96-well microtiter plate of microscopic grade (Microclear, Greiner Bio-one, France). The microtiter plates were then incubated at 20°C and observed under microscope at different time points. Bacteria were also enumerated as Colony-Forming Units (CFU) by recovering the gelled matrix from a well with a microstreaker and transferring it in a tube with 10 ml of sterile saline solution (9 g/L NaCl). The hydrogel was disrupted and homogenised by mechanical grinding with an Ika-Ultra-Turrax T25 (8000 t/min^{-1}) to fragment the microcolonies into dispersed cells. Following serial dilutions, samples were spread on petri dishes, incubated overnight and results expressed as CFU/ml.

Confocal Laser Scanning Microscopy (CLSM)

All microscopic observations were performed with a Leica HCS-SP8 confocal laser scanning microscope at the INRAE MIMA2 imaging platform (www6.jouy.inrae.fr/mima2). GFPmut2

(λ_{ex}485; λ_{em}508) and mRuby2 (λ_{ex}559; λ_{em}600) were excited respectively with laser bands 488 nm and 561 nm. A 40x water long range objective (numerical aperture = 0.8) was used with a 512 x 512 pixels definition (387 µm x 387 µm). Bidirectional acquisition speed of 600 Hz allows a frame rate of 2.3 images per second. For 3D stack analysis, a 1 µm step between z levels was used. For each condition, a minimum of 2 stacks in 4 different wells were acquired (8 z-stacks), except for co-cultures in 1.00 % LMPA where only 2 wells were analysed (4 z-stacks). For the tracking of swimming cells, 2 minutes time-lapse with one image every 459 ms is realised three times for each condition. Each microscopic image shown in the following results has a side (X/Y) of 387 µm and a height Z of 300.0 µm for a total volume of 45 046 875 μm^3 or 4.5 10^{-2} mm^3. For image analysis, all microscopic pictures were treated on IMARIS 9.64 (Bitplane, Switzerland). The raw fluorescence of each image was first binarised using the automated Imaris isosurface function. From binarised objects, it is possible to extract geometric parameters (*e.g.* biovolume, position, intensity, sphericity, speed) as raw data for further treatments in a data spreadsheet. For cell tracking in LMPA, observations in control, lactic acid and NaCl conditions were performed for both pathogens during 2 minutes timelapse to evaluate the motility radius. The effective radius of motility corresponds to a circle around a cell at a given time T_0, with the periphery of said circle being an estimate of the position of the bacteria at the time T_1.

Gels textural measurements

To assay the texture of gelled matrices, 30 ml of each hydrogels were prepared in 40 mL plastic cups (weight about 30 g, internal diameter 28 mm) and a TA.XT2 texture analyser (Stable Micro System) equipped with a 5 Kg load cell. Hydrogels were compressed using a flat disc (25 mm diameter, height 2 mm) pushing at a crosshead speed of 1 $mm.s^{-1}$ until a depth of 40 mm is reached (1.5 cm gap with bottom of cup). During compression, the normal force (N) increased linearly at a fast pace until it reached a plateau. The value of the average force of the plateau (FP, N) was used to calculate the rupture point (in weight, g) to represent the hardness of the sample.

Statistics

ANOVA variance analysis were realised with Statgraphics centurion (Statgraphics Technologies, Inc.) from 4 to 8 independent replicates. Differences were considered

significant when $P<0.05$ with P being the critical probability associated with the Fisher test. Graphs and heatmaps were performed with Prism 9 (Graphpad; CA, USA).

3) Results

3.1) Microcolony size and morphology are influenced by the initial load of the inoculum and LMPA concentration of the gelled matrices

To evaluate how initial bacterial load could affect spatial organisation and distribution of bacteria in gelled matrices, the size and morphology of in-gel bacterial microcolonies were assessed for initial concentrations ranging from 10^2 to 10^5 CFU/ml at a fixed LMPA concentration of 0.50 % (Figure 1).

Microcolonies in the gelled matrices generally appeared with spherical/ovoid shapes with a rougher form for *E. coli* O157:H7 compared to *L. monocytogenes* (Figures 1A and 1C). At low initial loads, scarce but large microcolonies were observed contrary to higher initial loads where microcolonies got smaller but more numerous (Figure 1A). Quantitative analysis demonstrated similar trends for both pathogens (Figure 1B). For initial load from 10^3 to 10^5 CFU/ml in 0.50 % LMPA, the mean biovolumes of microcolonies were 630 000 μm^3 and 15 000 μm^3, respectively, and inversely proportional with the initial load. For both pathogens, microcolonies tended to adopt a lentillar form associated with a reduced sphericity below an initial load of 10^3 CFU/ml (Figures 1A and 1C).

The effect of the concentration of jellifying agent on bacterial colonisation was further explored using different concentrations of LMPA (ranging from 0.25 % to 1.00 %) with an initial load of 10^5 CFU/ml (Figure 2). The morphology and distribution of bacterial cells changed significantly over the different concentrations tested, but the average number of cells per image was not significantly impacted (supplementary material Figure S1). With increasing LMPA concentrations, a shift from single cells to microcolonies was observed from and above 0.50 % LMPA (Figure 2). Between 0.50 % and 1.00 % LMPA, the biovolumes of microcolonies were significantly different and ranged from $1.0\ 10^2$ to $7.0\ 10^4$ μm^3 (Figure 2A and 2B). Investigating the effects on these pathogens in co-culture,

the overall size of microcolonies was significantly different compared to mono-culture conditions (Figure 2C). The mean values of 1.4 10^4 and 4.5 10^4 µm^3 for the biovolumes of *L. monocytogenes* and *E. coli* O157:H7 in mono-culture became 2.0 10^4 and 6.0 10^4 µm^3 in average for each pathogen in co-culture.

3.2) Bacterial growth in gelled matrices supplemented with lactic acid and NaCl

Considering lactic acid and/or NaCl can be found in food matrices subjected to contamination by *L. monocytogenes* or *E. coli* O157:H7, *e.g.* some meat or cheese products, their effect on bacterial colonisation was further considered by supplementing the gelled matrix with lactic acid and/or NaCl as described in the part "Materials and Methods". Besides CLSM examinations in these different conditions with various concentrations of LMPA, lactic acid and/or NaCl (Figure 3A), microcolonies were further quantitatively analysed regarding their bacterial biovolumes (Figure 3B). In this study, bacterial microcolonies were defined as detected objects larger than 10^3 µm^3. This threshold volume corresponds to a spherical object with a diameter of 20 µm, which was the lowest measurement for microcolonies in the control conditions.

At all LMPA concentrations with lactic acid, quantitative analysis yielded in a loss in microcolonies formation with a drop of objects mean biovolume from 10^4 µm^3 in gels without lactic acid to below 10^2 µm^3 for both *L. monocytogenes* and *E. coli* O157:H7 in presence of the acid (Figure 3). While *E. coli* O157:H7 was more resilient to lactic acid with a final population density of around 10^7 CFU/ml, it was significantly lower for *L. monocytogenes* with a decrease from 10^9 CFU/ml (control) to 10^5 CFU/ml (Figure 3, supplementary material Figure S2). Interestingly, in the presence of *E. coli* O157:H7, *L. monocytogenes* exhibited a better resilience to the effect of lactic acid by reaching a final density of 10^7 CFU/ml (Figures 3); on the contrary, *E. coli* O157:H7 appeared more severely impacted when in presence of *L. monocytogenes* compared to mono-culture conditions both in terms of microcolony formation and final cell density as both were lower then.

In presence of NaCl, the size of the microcolonies of *L. monocytogenes* was quite similar, *i.e.* around 10^3 µm^3, whatever the LMPA concentration tested (Figure 3). Of note, some cell aggregates could be observed on the verge of microcolony only at the lowest LMPA concentration (0.25 %). For *E. coli* O157:H7, there was no variation in the microcolonies size

but the population of single cells could not be observed anymore with salt supplementation (Figure 3). NaCl also appeared to promote adherence and biofilm development on the polystyrene at the bottom of the wells for both pathogens at 0.25 % LMPA (Figure 3, supplementary material Figure S3), as well as at 0.50 % LMPA but to a lesser extent (Figure 3). At 1.00 % LMPA concentration, however, no significant difference regarding microcolonies formation and adherence to the bottom of the wells could be observed compared to the control conditions. In the presence of NaCl in co-culture, the size of the microcolonies were significantly smaller (10^2 µm^3 instead of 10^4 µm^3) for *E. coli* O157:H7 at 48 h compared to mono-culture conditions (Figures 3, supplementary material Figure S4); at 96 h, however, the mean biovolumes were equivalent between mono- and co-culture conditions indicating that the expansion of microcolonies was only slowed down and temporarily delayed.

In gelled matrices supplemented with both lactic acid and NaCl, microcolonies were no longer observed for both *L. monocytogenes* and *E. coli* O157:H7 at all LMPA concentrations (Figure 3), with mean biovolumes (10^2 µm^3) comparable to what was seen in the lactic acid condition. Adherence and biofilm development at the bottom of the wells was still observed for *E. coli* O157:H7 with 0.25 % and 0.50 % LMPA, but not for *L. monocytogenes* (Figure 3, supplementary material Figure S3). However, for co-cultures in this condition containing lactic acid and NaCl, *L. monocytogenes* had a higher biovolume and formed a biofilm with *E. coli* O157:H7 at the bottom of the well (Figure 3, supplementary material Figure S3).

3.3) Single-cell motility of *L. monocytogenes* and *E. coli* O157:H7 in the gelled matrices

With no addition of lactic acid or NaCl, single cells motility were only observed in gelled matrices at 0.25 % LMPA with mean speeds (Vmean) of 0.53 µm/s and 0.68 µm/s for *E. coli* O157:H7 and *L. monocytogenes* respectively (Figure 4, supplementary material Figure S5). At higher LMPA concentrations bacterial cells were sessile and generally part of microcolonies (Figure 3). At 0.25 % LMPA supplemented with lactic acid, motility was observed for both pathogens. When it was 0.25 % LMPA supplemented with NaCl, *L. monocytogenes* was motile but not *E. coli* O157:H7. The same results were obtained at

0.50 % LMPA but lower speed rates were recorded. At 1.00 % LMPA, no motility was observed whatever the strain and the supplements (Figure 4).

In all tested conditions, the variation of Vmean values were less pronounced than for the maximum speed (Vmax) of the single cells. In the presence of lactic acid for *E. coli O157:*H7 and in the presence of NaCl for *L. monocytogenes* , there were clear shifts of the Vmax with significantly higher values than in other conditions (Figure 4, supplementary material Figure S5). For *E. coli* O157:H7 in presence of lactic acid, the Vmax were 2.7 and 2.4 µm/s at 0.25 % and 0.50 % LMPA, respectively (versus 1.27 and 0 µm/s with no supplementation) (supplementary material Figure S5). This increase in the cell motility upon NaCl or lactic acid supplementation was not observed anymore at 1.00 % LMPA. Those results are in accordance with the microscopic observations and motility tracking (Figure 6). For *L. monocytogenes*, Vmax reached 4.8 and 2.2 µm/s with NaCl supplementation at 0.25 % and 0.50 % LMPA, respectively (versus 1.6 and 0 µm/s with no supplementation) (supplementary material Figure S5).

Considering the distribution of the cell population, the two pathogens appeared to behave differently in conditions promoting cell motility (Figure 4); as most cells of *L. monocytogenes* reacted to lactic acid or NaCL supplementation, while only a small portion of *E. coli* O157:H7 cells did. With NaCl supplementation in gelled matrix, over 80 % of *L. monocytogenes* cells had Vmax higher than 2 µm/s in media NaCl, whereas 38 % of *E. coli* O157:H7 still had a Vmax below 1 µm/s with lactic acid (Figure 4). When both lactic acid and NaCl were added to the gelled matrices, the Vmean and Vmax for *L. monocytogenes* were not significantly different from the results obtained with the sole supplementation in lactic acid (Figure 4, supplementary material Figure S5). For *E. coli* O157:H7, motility was equivalent to what was observed in the control for 0.25 % and 0.50 % LMPA supplemented with lactic acid and NaCl (Figure 4).

In co-cultures, a slight but significant increase of Vmean for *L. monocytogenes* upon NaCl supplementation was observed (supplementary material Figure S6). In co-culture with lactic acid, the Vmean for *L. monocytogenes* was doubled in comparison to mono-culture conditions at 0.25 % and 0.50 % LMPA. For *E. coli* O157:H7 the opposite was observed with a general decreased in the Vmean values. Co-cultivation of *E. coli* O157:H7 and *L. monocytogenes* in gelled matrices thus led to significant change in the motility trends for each strain.

With the addition of lactic acid or NaCl in 0.50 % or 1.00 % LMPA gelled matrices, cell motility was promoted for both *L. monocytogenes* and *E. coli* O157:H7 (Figure 4). As this could result from variations in the hardness of the gelled matrices in these conditions, the texture of the gelled matrices was further considered (Figure 5). As expected, a significant increase in the hardness of the gelled matrices was confirmed with increasing LMPA concentrations (Figure 5); the gelled matrix was 5.5 times harder at 0.50 % LMPA and 14.5 times harder at 1.00 % LMPA compared to 0.25 % LMPA. When lactic acid or NaCl were added, the rheology of the gelled matrices was significantly modified as hydrogels composed of 0.50 % LMPA and supplemented with NaCl could support up to 795 g (i.e. a 33 % decrease in strength) and a gelled matrix at 0.50 % LMPA with lactic acid only 173 g (i.e. 89 % decrease in strength) compared to the control condition (gelled matrix with no supplementation). Also, variation in the hydrogel hardness could mainly explain the increase in cell motility for *L. monocytogenes* in gelled matrices with lactic acid. However, for a 0.50 % LMPA supplemented with NaCl, the Vmean and Vmax obtained for *L. monocytogenes* were significantly higher than at 0.25 % LMPA when the hydrogel hardness of the control condition was in fact lower (Figures 4 and 5, supplementary material Figure S5). Similar observations could apply for the Vmean and Vmax of *E. coli* O15:H7 at 0.50 % LMPA with lactic acid versus conditions at 0.25 % LMPA, where hydrogel hardness is equivalent but motility is not. In these conditions, variations of the cell motility would thus result from physiological adaptation of bacterial cells rather than from modifications in the texture of the gelled matrices.

In order to further characterise the cell motility of *L. monocytogenes* and *E. coli* O157:H7 in the different gelled matrix conditions, the effective radius of motility for each bacterial cell was evaluated. At 0.25 % LMPA, where *L. monocytogenes* and *E. coli* O157:H7 were less motile, the same effective radius of ~2.5 µm/m was measured (Figure 6, supplementary material Figure S7 video A and D). With the addition of lactic acid, an increase in the cellular speed was observed for both pathogens (Figure 4) and tumbling was also observed (Figure 6, supplementary material Figure S7 video B and E); the effective radii in this condition were about 7.5 µm/m and 12.5 µm/m for *L. monocytogenes* and *E. coli* O157:H7 respectively. In gelled matrices supplemented with NaCl, no motility could be observed for *E. coli* O157:H7, whereas *L. monocytogenes* had a mean effective radius of 31.8 µm/m (Figure 6, supplementary material Figure S7 video C and F). This increase in effective radius is observed for *L. monocytogenes* with or without supplementation with NaCl with no increase

in the Vmean (0.68 µm/s) but a significant change in Vmax (from 1.57 to 4.77 µm/s) (supplementary material Figure S5).

4) Discussion

Food matrixes are rich media harbouring hundreds of microbial species (Chaillou et al., 2015; Yu et al., 2019) and understanding the behaviour of foodborne pathogens in this environment is one of the key prerequisite to refine risk assessment models and to ultimately improve microbiological food safety (Koutsoumanis et al., 2016; Membré and Guillou, 2016). Though, behaviours of bacterial foodborne pathogens are generally assessed in liquid growth media that are poorly mimicking food matrices. At the same time, food matrices are often opaque, preventing direct photonic microscopic observation of these microorganisms to evaluate their physiology and behaviour. To alleviate this limitation, genetically fluorescent *L. monocytogenes* and *E. coli* O157:H7 were grown in transparent nutritive gelled matrices for *in situ* observations by CSLM (Bridier et al., 2015; Verheyen et al., 2019). Besides the visualisation of bacterial cells in the gelled matrix, the use of LMPA presented the advantages of a low solidification point (~25°C) limiting bacterial thermal stress, combined to a low melting point (≤65°C) facilitating the experimental handling compared to other jellifying agents such as agar, guar gum or gelatin (Jaeger et al., 2015). Furthermore, LMPA allowed to cover a wide range of textures relevant to various food matrices, *e.g.* 0.50 % LMPA presented a hardness similar to fried beef patties (Uriyapongson, 2007) or 1.00 % LMPA was comparable to the texture of mature cheddar (Pollard et al., 2003).

In most conditions tested in the gelled matrices, bacterial colonised the media as microcolonies adopting a spherical morphology. While similar observations where already reported in gelatin gels and/or for other bacterial species (Antwi et al., 2006; Mitchell and Wimpenny, 1997), in this investigation a clear inverted correlation between the density of founder cells and the radius of the microcolonies was highlighted. While giant microcolonies could be observed at lowest rates of initial inoculation rate (*e.g.* radius of about 110 µm at 10^2 CFU/ml), the distances between microcolonies decreased as the initial inoculation rate increased (*e.g.* from one millimeter to around 80 µm). Modification of metabolite gradient in the microcolonies can be expected between those conditions (Jeanson et al., 2015). In addition, the sphericity of the microcolonies increased with the initial concentration of the

inoculum, whereas more oblate/lentillar shapes were observed at the lowest initial load. Such lentillar microcolonies morphology were previously reported but as a result of increasing concentrations of gelatin (Antwi et al., 2006) or agarose (Zhang et al., 2021).

The formation of microcolonies is a food safety issue due to emerging properties caused by heterogeneity and diversification of bacterial phenotypes as colonies age (Saint-Ruf et al., 2014); quorum sensing (Garmyn et al., 2011; Ji et al., 1995; Kanamaru et al., 2000); or long term consequences on virulence in host (Kortebi et al., 2017; Travier et al., 2013). Supplementation of the gelled matrices in lactic acid and/or NaCl had profound effects on microcolonies development of both pathogens. The final cell density of *E. coli* O157:H7 and *L. monocytogenes* as well as microcolony formation was significantly reduced in the presence of lactic acid and most certainly result from cumulative inhibitory effects of pH and diffusion of undissociated weak acid form across the cellular membranes (Arcari et al., 2020; Booth, 1985; Lambert and Stratford, 1999; Russell and Cook, 1995). The supplementation with NaCl in tested hydrogels did not significantly impacted the final cell density but a modification of the spatial distribution in the gelled matrix was observed, especially development at the bottom of the wells. Addition of NaCl was previously shown to influence the physiology, including bacterial adhesion and/or biofilm formation abilities of *E. coli* (Cerca and Jefferson, 2008; Hou et al., 2014; Olesen and Jespersen, 2010) or *L. monocytogenes* (Lee et al., 2019; Olesen et al., 2009; Silva et al., 2020; Xu et al., 2010) in various growth conditions.

Interestingly, the behaviours of *L. monocytogenes* and *E. coli* O157:H7 appeared to be influenced when they were co-cultured. While generally considered in discrete manner whenever in food safety (from quality control to risk modelling) or in medical microbiology (in case of human infections), these zoonotic foodborne bacterial pathogens can co-occur and contaminate the same foodstuffs, especially some types of cheese and meat as well as some vegetables products (Fantelli and Stephan, 2001; Kallipolitis et al., 2020; Lin et al., 1996; Luna-Guevara et al., 2019) and possibility of co-infection should not be overlooked (Opperman and Bamford, 2018).

Cell motility appeared to be dependent on the texture of gelled matrix but also on the presence of lactic acid and/or NaCl. As expected, the speed of swimming in gelled matrices was slower than the one reported in liquid broth (Swiecicki et al., 2013) and would rather correspond to speed rate measured at the edge of swarming colonies (Damton et al., 2010). Besides the speed rate, lactic acid is known to have an impact on the rotation of the flagella in *E. coli* as it

induces inversion of flagellar rotation from counter-clockwise (CCW) to clockwise (CW) (Xu et al., 2019); CCW rotation is generally associated with straight swimming whereas CW rotation of the flagella results in tumbling behaviour in *E. coli* (Larsen et al., 1974). *E. coli* generally do not express motility at low pH but a bacteriophage of *E. coli* O157:H7 has been demonstrated to induce a swarming phenotype in acidic media (Su et al., 2010). In *L. monocytogenes*, the expression of flagella is known to be repressed in the presence of lactic acid (Cortes et al., 2020) as well as by high concentration of NaCl (Caly et al., 2009). In both *E. coli* and *L. monocytogenes,* "hopping" and "trapping" behaviour could also contribute to cell motility and occur as observed in porous matrices, where short bursts of free movement are responsible for most of the apparent motility (Bhattacharjee and Datta, 2019).

Investigation of bacterial colonisation in a model of gelled food matrices by bacterial foodborne pathogens demonstrated a wide range of colonisation patterns depending on environmental conditions. Different strains of a same species, including *E. coli* O157:H7 or *L. monocytogenes,* can exhibit different behaviours and phenotypes (Biscola et al., 2011; Borucki et al., 2003; Orsi et al., 2011; Renter et al., 2003), but the diversification of cell types in spatially organised communities can triggers emerging community properties. Further layers of complexity can be added by biocoenoses forming discrete microecosystems where foodborne pathogens interact with other species of the food microbiota; as well as various regulatory and molecular mechanisms including phase variation (e.g. sequences inversions, different methylation sites and levels of methylase expression) or bistability of gene expression (Ackermann, 2015; Veening et al., 2008). While the present investigation highlighted some differences in the spatial organisation of some key foodborne pathogens in gelled matrices, the integration of the different levels of heterogeneity in food matrices is clearly the next frontiers in the improvement of risk assessment of microbial food safety and necessitate to consider the foodborne pathogen at a single cell level besides the population level classically considered in food matrices (Lianou and Koutsoumanis, 2013). Besides description of growth parameters, reaching this aim will require to acquire in-depth knowledge of molecular mechanisms at play in the phenotypic heterogeneity and combine it to mathematical modelling of the behaviour of foodborne pathogens.

Declaration of competitive interest

None

Acknowledgments

This work received funding from the French government through the grant "ANR 17-CE21-0002". The partners of the ANR "PathoFood" are acknowledged for fruitful discussions about *L. monocytogenes* and *E. coli* O157:H7 behaviour in food matrices. Julien Deschamps (INRAE) is warmly acknowledged for assistance with Confocal Laser Scanning Microscopy.

References

Ackermann, M., 2015. A functional perspective on phenotypic heterogeneity in microorganisms. Nat. Rev. Microbiol. 130, 8 497-508 https://doi.org/10.1038/nrmicro3491

Ageorges, V., Schiavone, M., Jubelin, G., Caccia, N., Ruiz, P., Chafsey, I., Bailly, X., Dague, E., Leroy, S., Paxman, J., Heras, B., Chaucheyras-Durand, F., Rossiter, A.E., Henderson, I.R., Desvaux, M., 2019. Differential homotypic and heterotypic interactions of antigen 43 (Ag43) variants in autotransporter-mediated bacterial autoaggregation. Sci. Rep. 9, article 11100, 19 pp. https://doi.org/10.1038/s41598-019-47608-4

Antwi, M., Geeraerd, A.H., Vereecken, K.M., Jenné, R., Bernaerts, K., Van Impe, J.F., 2006. Influence of a gel microstructure as modified by gelatin concentration on Listeria innocua growth. Innov. Food Sci. Emerg. Technol. 7, 124–131. https://doi.org/10.1016/j.ifset.2005.08.001

Arcari, T., Feger, M.-L., Guerreiro, D.N., Wu, J., O'Byrne, C.P., 2020. Comparative Review of the Responses of Listeria monocytogenes and Escherichia coli to Low pH Stress. Genes (Basel). 11, 1330. https://doi.org/10.3390/genes11111330

Bhattacharjee, T., Datta, S.S., 2019. Bacterial hopping and trapping in porous media. Nat.

Commun. 10. article 2075, 9 pp. https://doi.org/10.1038/s41467-019-10115-1

Biscola, F.T., Abe, C.M., Guth, B.E.C., 2011. Determination of adhesin gene sequences in, and biofilm formation by, O157 and non-O157 Shiga toxin-producing Escherichia coli strains isolated from different sources. Appl. Environ. Microbiol. 77, 2201–2208. https://doi.org/10.1128/AEM.01920-10

Booth, I.R., 1985. Regulation of cytoplasmic pH in bacteria. Microbiol. Rev. 49, 4 359-378 https://doi.org/10.1128/mmbr.49.4.359-378.1985

Borucki, M.K., Peppin, J.D., White, D., Loge, F., Call, D.R., 2003. Variation in Biofilm Formation among Strains of Listeria monocytogenes. Appl. Environ. Microbiol. 69, 7336–7342. https://doi.org/10.1128/AEM.69.12.7336-7342.2003

Bridier, A., Hammes, F., Canette, A., Bouchez, T., Briandet, R., 2015. Fluorescence-based tools for single-cell approaches in food microbiology. Int. J. Food Microbiol. 213, 2–16. https://doi.org/10.1016/j.ijfoodmicro.2015.07.003

Caly, D., Takilt, D., Lebret, V., Tresse, O., 2009. Sodium chloride affects Listeria monocytogenes adhesion to polystyrene and stainless steel by regulating flagella expression. Lett. Appl. Microbiol. 49, 751–756. https://doi.org/10.1111/j.1472-765X.2009.02735.x

Caniça, M., Manageiro, V., Abriouel, H., Moran-Gilad, J., Franz, C.M.A.P., 2019. Antibiotic resistance in foodborne bacteria. Trends Food Sci. Technol. 84, 41-44 https://doi.org/10.1016/j.tifs.2018.08.001

Cerca, N., Jefferson, K.K., 2008. Effect of growth conditions on poly-N-acetylglucosamine expression and biofilm formation in Escherichia coli. FEMS Microbiol. Lett. 283, 36–41. https://doi.org/10.1111/j.1574-6968.2008.01142.x

Chaillou, S., Chaulot-Talmon, A., Caekebeke, H., Cardinal, M., Christieans, S., Denis, C., Hélène Desmonts, M., Dousset, X., Feurer, C., Hamon, E., Joffraud, J.J., La Carbona, S., Leroi, F., Leroy, S., Lorre, S., Macé, S., Pilet, M.F., Prévost, H., Rivollier, M., Roux, D., Talon, R., Zagorec, M., Champomier-Vergès, M.C., 2015. Origin and ecological selection of core and food-specific bacterial communities associated with meat and seafood spoilage. ISME J. 9, 1105–1118. https://doi.org/10.1038/ismej.2014.202

Cormack, B.P., Valdivia, R.H., Falkow, S., 1996. FACS-optimized mutants of the green fluorescent protein (GFP), in: Gene. Elsevier B.V., pp. 33–38. https://doi.org/10.1016/0378-1119(95)00685-0

Cortes, B.W., Naditz, A.L., Anast, J.M., Schmitz-Esser, S., 2020. Transcriptome Sequencing of Listeria monocytogenes Reveals Major Gene Expression Changes in Response to Lactic Acid Stress Exposure but a Less Pronounced Response to Oxidative Stress. Front. Microbiol. 10, article 3110, 14 pp. https://doi.org/10.3389/fmicb.2019.03110

Costello, K.M., Gutierrez-Merino, J., Bussemaker, M., Ramaioli, M., Baka, M., Van Impe, J.F., Velliou, E.G., 2018. Modelling the microbial dynamics and antimicrobial resistance development of Listeria in viscoelastic food model systems of various structural complexities. Int. J. Food Microbiol. 286, 15–30. https://doi.org/10.1016/j.ijfoodmicro.2018.07.011

Cussler, E.L. (Cambridge U., 1997. Diffusion: Mass Transfer in Fluid Systems, 2nd editio. ed. Cambridge University Press. Part of Cambridge Series in Chemical Engineering.

Damton, N.C., Turner, L., Rojevsky, S., Berg, H.C., 2010. Dynamics of bacterial swarming. Biophys. J. 98, 2082–2090. https://doi.org/10.1016/j.bpj.2010.01.053

EFSA and ECDC (European Food Safety Authority and European Centre for Disease Prevention and Control), 2021. The European Union One Health 2019 Zoonoses Report. EFSA Journal 2021;19(2):6406, 286 pp. ISSN: 1831-4732 https://doi.org/10.2903/j.efsa.2021.6406

Fantelli, K., Stephan, R., 2001. Prevalence and characteristics of Shigatoxin-producing Escherichia coli and Listeria monocytogenes strains isolated from minced meat in Switzerland. Int. J. Food Microbiol. 70, 63–69. https://doi.org/10.1016/S0168-1605(01)00515-3

Fortineau, N., Trieu-Cuot, P., Gaillot, O., Pellegrini, E., Berche, P., Gaillard, J.L., 2000. Optimization of green fluorescent protein expression vectors for in vitro and in vivo detection of Listeria monocytogenes. Res. Microbiol. 151, 353–360. https://doi.org/10.1016/S0923-2508(00)00158-3

Garmyn, D., Gal, L., Briandet, R., Guilbaud, M., Lemaître, J.P., Hartmann, A., Piveteau, P.,

2011. Evidence of autoinduction heterogeneity via expression of the agr system of Listeria monocytogenes at the single-cell level. Appl. Environ. Microbiol. 77, 6286–6289. https://doi.org/10.1128/AEM.02891-10

Glaser, P., Frangeul, L., Buchrieser, C., Rusniok, C., Amend, A., Baquero, F., Berche, P., Bloecker, H., Brandt, P., Chakraborty, T., Charbit, A., Chetouani, F., Couvé, E., de Daruvar, A., Dehoux, P., Domann, E., Domínguez-Bernal, G., Duchaud, E., Durant, L., Dussurget, O., Entian, K.-D., Fsihi, H., Portillo, F.G.-D., Garrido, P., Gautier, L., Goebel, W., Gómez-López, N., Hain, T., Hauf, J., Jackson, D., Jones, L.-M., Kaerst, U., Kreft, J., Kuhn, M., Kunst, F., Kurapkat, G., Madueño, E., Maitournam, A., Vicente, J.M., Ng, E., Nedjari, H., Nordsiek, G., Novella, S., de Pablos, B., Pérez-Diaz, J.-C., Purcell, R., Remmel, B., Rose, M., Schlueter, T., Simoes, N., Tierrez, A., Vázquez-Boland, J.-A., Voss, H., Wehland, J., Cossart, P., 2001. Comparative Genomics of Listeria Species. Science 294 (5543) 849-852 doi: 10.1126/science.1063447.

Gobert, A.P., Vareille, M., Glasser, A.-L., Hindré, T., de Sablet, T., Martin, C., 2007. Shiga Toxin Produced by Enterohemorrhagic Escherichia coli Inhibits PI3K/NF-κB Signaling Pathway in Globotriaosylceramide-3-Negative Human Intestinal Epithelial Cells . J. Immunol. 178, 8168–8174. https://doi.org/10.4049/jimmunol.178.12.8168

Hou, B., Meng, X.R., Zhang, L.Y., Tan, C., Jin, H., Zhou, R., Gao, J.F., Wu, B., Li, Z.L., Liu, M., Chen, H.C., Bi, D.R., Li, S.W., 2014. TolC Promotes ExPEC Biofilm Formation and Curli Production in Response to Medium Osmolarity. Biomed Res. Int. 2014. article ID 574274, 10 pp. https://doi.org/10.1155/2014/574274

Jaeger, P.A., McElfresh, C., Wong, L.R., Ideker, T., 2015. Beyond agar: Gel substrates with improved optical clarity and drug efficiency and reduced autofluorescence for microbial growth experiments. Appl. Environ. Microbiol. 81, 5639–5649. https://doi.org/10.1128/AEM.01327-15

Jeanson, S., Floury, J., Gagnaire, V., Lortal, S., Thierry, A., 2015. Bacterial Colonies in Solid Media and Foods: A Review on Their Growth and Interactions with the Micro-Environment. Front. Microbiol. 6. article 1284, 20 pp https://doi.org/10.3389/fmicb.2015.01284

Ji, G., Beavis, R.C., Novick, R.P., 1995. Cell density control of staphylococcal virulence

mediated by an octapeptide pheromone. Proc. Natl. Acad. Sci. U. S. A. 92, 12055-12059. https://doi.org/10.1073/pnas.92.26.12055

Kabanova, N., Stulova, I., Vilu, R., 2012. Microcalorimetric study of the growth of bacterial colonies of Lactococcus lactis IL1403 in agar gels. Food Microbiol. 29, 67–79. https://doi.org/10.1016/j.fm.2011.08.018

Kallipolitis, B., Gahan, C.G., Piveteau, P., 2020. Factors contributing to Listeria monocytogenes transmission and impact on food safety. Curr. Opin. Food Sci. 36 9-17 https://doi.org/10.1016/j.cofs.2020.09.009

Kanamaru, Kyoko, Kanamaru, Kengo, Tatsuno, I., Tobe, T., Sasakawa, C., 2000. SdiA, an Escherichia coil homologue of quorum-sensing regulators, controls the expression of virulence factors in enterohaemorrhagic Escherichia coli O157:H7. Mol. Microbiol. 38, 805–816. https://doi.org/10.1046/j.1365-2958.2000.02171.x

Kortebi, M., Milohanic, E., Mitchell, G., Péchoux, C., Prevost, M.C., Cossart, P., Bierne, H., 2017. Listeria monocytogenes switches from dissemination to persistence by adopting a vacuolar lifestyle in epithelial cells. PLoS Pathog. 13 (11): e1006734. https://doi.org/10.1371/journal.ppat.1006734

Koutsoumanis, K.P., Lianou, A., Gougouli, M., 2016. Last developments in foodborne pathogens modeling. Curr. Opin. Food Sci. 8, 89-98 https://doi.org/10.1016/j.cofs.2016.04.006

Lambert, R.J., Stratford, M., 1999. Weak-acid preservatives: modelling microbial inhibition and response. J. Appl. Microbiol. 86, 157–164. https://doi.org/10.1046/j.1365-2672.1999.00646.x

Larsen, S.H., Reader, R.W., Kort, E.N., Tso, W.W., Adler, J., 1974. Change in direction of flagellar rotation is the basis of the chemotactic response in Escherichia coli. Nature 249, 74–77. https://doi.org/10.1038/249074a0

Lee, B.H., Cole, S., Badel-Berchoux, S., Guillier, L., Felix, B., Krezdorn, N., Hébraud, M., Bernardi, T., Sultan, I., Piveteau, P., 2019. Biofilm Formation of Listeria monocytogenes Strains Under Food Processing Environments and Pan-Genome-Wide Association Study. Front. Microbiol. 10, article 2698, 18 pp. https://doi.org/10.3389/fmicb.2019.02698

Lianou, A., Koutsoumanis, K.P., 2013. Strain variability of the behavior of foodborne bacterial pathogens: A review. Int. J. Food Microbiol. 137, 3 310-321 https://doi.org/10.1016/j.ijfoodmicro.2013.09.016

Licata, N.A., Mohari, B., Fuqua, C., Setayeshgar, S., 2016. Diffusion of Bacterial Cells in Porous Media. Biophys. J. 110, 247–257. https://doi.org/10.1016/j.bpj.2015.09.035

Lin, C. min, Fernando, S.Y., Wei, C. i., 1996. Occurrence of Listeria monocytogenes. Salmonella spp., Escherichia coli and E. coli O157:H7 in vegetable salads. Food Control 7, 135–140. https://doi.org/10.1016/0956-7135(96)00019-9

Lobete, M.M., Fernandez, E.N., Van Impe, J.F.M., 2015. Recent trends in non-invasive in situ techniques to monitor bacterial colonies in solid (model) food. Front. Microbiol. 6, article 148 9 pp. https://doi.org/10.3389/fmicb.2015.00148

Luna-Guevara, J.J., Arenas-Hernandez, M.M.P., Martínez De La Peña, C., Silva, J.L., Luna-Guevara, M.L., 2019. The Role of Pathogenic E. coli in Fresh Vegetables: Behavior, Contamination Factors, and Preventive Measures. Int. J. Microbiol. Article ID 2894328 10 pp, SN 1687-918X. https://doi.org/10.1155/2019/2894328

Membré, J.M., Guillou, S., 2016. Lastest developments in foodborne pathogen risk assessment. Curr. Opin. Food Sci. 8 120-126 https://doi.org/10.1016/j.cofs.2016.04.011

Mitchell, A.J., Wimpenny, J.W.T., 1997. The effects of agar concentration on the growth and morphology of submerged colonies of motile and non-motile bacteria. J. Appl. Microbiol. 83, 76–84. https://doi.org/10.1046/j.1365-2672.1997.00192.x

Nielsen, M.B., Knudsen, G.M., Danino-Appleton, V., Olsen, J.E., Thomsen, L.E., 2013. Comparison of heat stress responses of immobilized and planktonic Salmonella enterica serovar Typhimurium. Food Microbiol. 33, 221–227. https://doi.org/10.1016/j.fm.2012.09.020

Olesen, I., Jespersen, L., 2010. Relative gene transcription and pathogenicity of enterohemorrhagic Escherichia coli after long-term adaptation to acid and salt stress. Int. J. Food Microbiol. 141, 248–253. https://doi.org/10.1016/j.ijfoodmicro.2010.05.019

Olesen, I., Vogensen, F.K., Jespersen, L., 2009. Gene transcription and virulence potential of

Listeria monocytogenes strains after exposure to acidic and NaCl stress. Foodborne Pathog. Dis. 6, 669–680. https://doi.org/10.1089/fpd.2008.0243

Opperman, C.J., Bamford, C., 2018. Co-infection with Streptococcus pneumoniae and Listeria monocytogenes in an immunocompromised patient. South African Med. J. 108, 386–388. https://doi.org/10.7196/SAMJ.2018.v108i5.12957

Orsi, R.H., Bakker, H.C. de., Wiedmann, M., 2011. Listeria monocytogenes lineages: Genomics, evolution, ecology, and phenotypic characteristics. Int. J. Med. Microbiol. 301, (2) 79-96 https://doi.org/10.1016/j.ijmm.2010.05.002

Pin, C., Sutherland, J.P., Baranyi, J., 1999. Validating predictive models of food spoilage organisms. J. Appl. Microbiol. 87, 491–499. https://doi.org/10.1046/j.1365-2672.1999.00838.x

Pollard, A., Sherkat, F., Seuret, M.G., Halmos, A.L., 2003. Textural Changes of Natural Cheddar Cheese During the Maturation Process. J. Food Sci. 68, 2011–2016. https://doi.org/10.1111/j.1365-2621.2003.tb07010.x

Renier, S., Chagnot, C., Deschamps, J., Caccia, N., Szlavik, J., Joyce, S.A., Popowska, M., Hill, C., Knøchel, S., Briandet, R., Hébraud, M., Desvaux, M., 2014. Inactivation of the SecA2 protein export pathway in *Listeria monocytogenes* promotes cell aggregation, impacts biofilm architecture and induces biofilm formation in environmental condition. Environ. Microbiol. 16, 1176–1192. https://doi.org/10.1111/1462-2920.12257

Renter, D.G., Sargeant, J.M., Oberst, R.D., Samadpour, M., 2003. Diversity, frequency, and persistence of Escherichia coli O157 strains from range cattle environments. Appl. Environ. Microbiol. 69, 542–547. https://doi.org/10.1128/AEM.69.1.542-547.2003

Ribeiro, A.C.F., Lobo, V.M.M., Leaist, D.G., Natividade, J.J.S., Veríssimo, L.P., Barros, M.C.F., Cabral, A.M.T.D.P.V., 2005. Binary diffusion coefficients for aqueous solutions of lactic acid. J. Solution Chem. 34, 1009–1016. https://doi.org/10.1007/s10953-005-6987-3

Russell, J.B., Cook, G.M., 1995. Energetics of bacterial growth: balance of anabolic and catabolic reactions. Microbiol. Rev. 59, 48–62. https://doi.org/10.1128/mr.59.1.48-62.1995

Saint-Ruf, C., Garfa-Traoré, M., Collin, V., Cordier, C., Franceschi, C., Matic, I., 2014. Massive diversification in aging colonies of Escherichia coli. J. Bacteriol. 196, 3059–3073. https://doi.org/10.1128/JB.01421-13

Silva, D.A.L., Tavares, R.M., Nero, L.A., 2020. Interference of sanitizers, NaCl and curing salts on *Listeria monocytogenes* adhesion and subsequent biofilm formation. Lett. Appl. Microbiol. 71, 438–443. https://doi.org/10.1111/lam.13374

Silva, J.V.C., Peixoto, P.D.S., Lortal, S., Floury, J., 2013. Transport phenomena in a model cheese: The influence of the charge and shape of solutes on diffusion. J. Dairy Sci. 96, 6186–6198. https://doi.org/10.3168/jds.2013-6552

Skandamis, P.N., Jeanson, S., 2015. Colonial vs. planktonic type of growth: Mathematical modeling of microbial dynamics on surfaces and in liquid, semi-liquid and solid foods. Front. Microbiol. 6, article 1178. https://doi.org/10.3389/fmicb.2015.01178

Smith, S., Schaffner, D.W., 2004. Evaluation of a Clostridium perfringens predictive model, developed under isothermal conditions in broth, to predict growth in ground beef during cooling. Appl. Environ. Microbiol. 70, 2728–2733. https://doi.org/10.1128/AEM.70.5.2728-2733.2004

Stewart, P.S., Franklin, M.J., 2008. Physiological heterogeneity in biofilms. Nat. Rev. Microbiol. 6 199–210 https://doi.org/10.1038/nrmicro1838

Su, L.K., Lu, C.P., Wang, Y., Cao, D.M., Sun, J.H., Yan, Y.X., 2010. Lysogenic infection of a Shiga toxin 2-converting bacteriophage changes host gene expression, enhances host acid resistance and motility. Mol. Biol. 44, 54–66. https://doi.org/10.1134/S0026893310010085

Swiecicki, J.M., Sliusarenko, O., Weibel, D.B., 2013. From swimming to swarming: Escherichia coli cell motility in two-dimensions. Integr. Biol. (United Kingdom) 5, 1490–1494. https://doi.org/10.1039/c3ib40130h

Theys, T.E., Geeraerd, A.H., Van Impe, J.F., 2009. Evaluation of a mathematical model structure describing the effect of (gel) structure on the growth of listeria innocua, lactococcus lactis and salmonella typhimurium. J. Appl. Microbiol. 107, 775–784. https://doi.org/10.1111/j.1365-2672.2009.04256.x

Theys, T.E., Geeraerd, A.H., Verhulst, A., Poot, K., Van Bree, I., Devlieghere, F., Moldenaers, P., Wilson, D., Brocklehurst, T., Van Impe, J.F., 2008. Effect of pH, water activity and gel micro-structure, including oxygen profiles and rheological characterization, on the growth kinetics of *Salmonella Typhimurium*. Int. J. Food Microbiol. 128, 67–77. https://doi.org/10.1016/j.ijfoodmicro.2008.06.031

Travier, L., Guadagnini, S., Gouin, E., Dufour, A., Chenal-Francisque, V., Cossart, P., Olivo-Marin, J.C., Ghigo, J.M., Disson, O., Lecuit, M., 2013. ActA Promotes Listeria monocytogenes Aggregation, Intestinal Colonization and Carriage. PLoS Pathog. 9(1): e1003131. https://doi.org/10.1371/journal.ppat.1003131

Uriyapongson, J., 2007. Comparison and improvement of chemical and physical characteristics of low- fat ground beef and buffalo meat patties at frozen storage. Ital. J. Anim. Sci. 6, 1171–1174. https://doi.org/10.4081/ijas.2007.s2.1171

Uyttendaele, M., Busschaert, P., Valero, A., Geeraerd, A.H., Vermeulen, A., Jacxsens, L., Goh, K.K., De Loy, A., Van Impe, J.F., Devlieghere, F., 2009. Prevalence and challenge tests of Listeria monocytogenes in Belgian produced and retailed mayonnaise-based deli-salads, cooked meat products and smoked fish between 2005 and 2007. Int. J. Food Microbiol. 133, 94–104. https://doi.org/10.1016/j.ijfoodmicro.2009.05.002

Veening, J.-W., Smits, W.K., Kuipers, O.P., 2008. Bistability, Epigenetics, and Bet-Hedging in Bacteria. Annu. Rev. Microbiol. 62, 193–210. https://doi.org/10.1146/annurev.micro.62.081307.163002

Verheyen, D., Baka, M., Akkermans, S., Skåra, T., Van Impe, J.F., 2019. Effect of microstructure and initial cell conditions on thermal inactivation kinetics and sublethal injury of Listeria monocytogenes in fish-based food model systems. Food Microbiol. 84 article 103267 14 pp, ISSN 0740-0020. https://doi.org/10.1016/j.fm.2019.103267

Xu, H., Zou, Y., Lee, H.-Y., Ahn, J., 2010. Effect of NaCl on the Biofilm Formation by Foodborne Pathogens. J. Food Sci. 75, M580–M585. https://doi.org/10.1111/j.1750-3841.2010.01865.x

Xu, J., Koyanagi, Y., Isogai, E., Nakamura, S., 2019. Effects of fermentation products of the commensal bacterium Clostridium ramosum on motility, intracellular pH, and flagellar synthesis of enterohemorrhagic Escherichia coli. Arch. Microbiol. 201, 841–846.

https://doi.org/10.1007/s00203-019-01656-6

Yang, A., Tang, W.S., Si, T., Tang, J.X., 2017. Influence of Physical Effects on the Swarming Motility of Pseudomonas aeruginosa. Biophys. J. 112, 1462–1471. https://doi.org/10.1016/j.bpj.2017.02.019

Yu, Z., Peruzy, M.F., Dumolin, C., Joossens, M., Houf, K., 2019. Assessment of food microbiological indicators applied on poultry carcasses by culture combined MALDI-TOF MS identification and 16S rRNA amplicon sequencing. Food Microbiol. 82, 53–61. https://doi.org/10.1016/j.fm.2019.01.018

Zhang, Q., Li, J., Nijjer, J., Lu, H., Kothari, M., Alert, R., Cohen, T., Yan, J., 2021. Morphogenesis and cell ordering in confined bacterial biofilms. Proc. Natl. Acad. Sci. 118 (31), e2107107118. https://doi.org/10.1073/pnas.2107107118

Figure legends

Figure 1: Effect of the bacterial initial load on the spatial distribution, biovolume and morphology of microcolonies of *L. monocytogenes* and *E. coli* O157:H7 in gelled matrices. A: CLSM observations of *L. monocytogenes* (green) and *E. coli* O157:H7 (red) at 0.50 % LMPA for different bacterial initial loads after 96h of growth at 20°C. Representative pictures correspond to microcolonies isosurfaces after fluorescence segmentation. B: Mean biovolume in $\log_{10}$ (μm^3) of microcolonies at 96 h at different bacterial initial loads. C: Mean sphericity of microcolonies at different bacterial initial loads. Error bars indicate the mean standard deviation.

Figure 2: Effect of gelled matrices LMPA concentration on microcolonies formation by *L. monocytogenes* and *E. coli* O157:H7. CLSM observations of mono-cultures of *L. monocytogenes* (A, green) and *E. coli* O157:H7 (B, red), as well as co-cultures (C-C) of both pathogens at 20°C and 96 h. Representative hydrogel sections correspond to 387x387x300 µm.

Figure 3: Impact of NaCl and/or lactic acid supplementation on microcolonies of *L. monocytogenes* and *E. coli* O157:H7 in gelled matrices. A: CLSM observations of genetically fluorescent *L. monocytogenes* (green) and *E. coli* O157:H7 (red) cells in gelled matrices with different LMPA concentrations (0.25, 0.50 or 1.00 %) *(i)* without the addition of lactic acid or NaCl (control condition), *(ii)* with the addition of lactic acid, *(iii)* with supplementation NaCl, or *(iv)* with both lactic acid and NaCl, in mono- and co-cultures at 96 h. B: Heatmap of the mean biovolume of microcolonies in the different gelled matrix conditions. The colour scale is expressed in $\log_{10}$ (μm^3) with cooler tones indicating small microcolonies and warmer colours are attributed to large microcolonies. Data originate from CSLM observations performed at 48 h and 96 h from mono-culture (M-C) and co-culture (C-C) conditions. A threshold of 10^3 μm^3 is set as the limit between single cells or small aggregates and microcolonies.

Figure 4: Quantitative analysis of individual cell motility of *L. monocytogenes* and *E. coli* O157:H7 in different gelled matrix conditions. The mean speed (Vmean in red) and the max speed (Vmax in blue) were calculated from bacterial cell observations in time-lapse microscopy as described in the Material and Methods section. From there, the percentage of population for the different speed values was represented as a density bar. The averages for

the Vmean and Vmax were further calculated and represented as bright colour lines (red and blue respectively) to highlight shift in motility of the cell population. Gelled matrices were obtained at different LMPA concentrations (i.e. 0.25 %, 0.50 % or 1.00 %) *(i)* without the addition of lactic acid or NaCl (control condition), *(ii)* with the addition lactic acid, *(iii)* with supplementation of NaCl, or *(iv)* with both lactic acid and NaCl.

Figure 5: Texture of the gelled matrices supplemented with lactic acid or NaCl. Mean of hydrogel hardness (g) at the different LMPA concentrations considered: 1.00 %, 0.50 % and 0.25 %, without supplementation (control condition in black) or supplemented with Lactic acid (green) or with NaCl (orange). Error bars indicate the standard deviation (calculated from 10 measurements).

Figure 6: Time-tracking of single cells motility of *L. monocytogenes* (A, B, C) and *E. coli* O157:H7 (D, E, F) in gelled media. Data acquisition was performed at 0.25 % LMPA; (A, D) without the addition of lactic acid or NaCl (control condition); (B, E) with the addition of lactic acid, or (C, F) with supplementation of NaCl. Tracks were acquired and represented over the full duration of the timelapse (120 s). All images are 101 µm by 82 µm and correspond to close up of images found in the 6 supplementary material movies V7A to V7F.

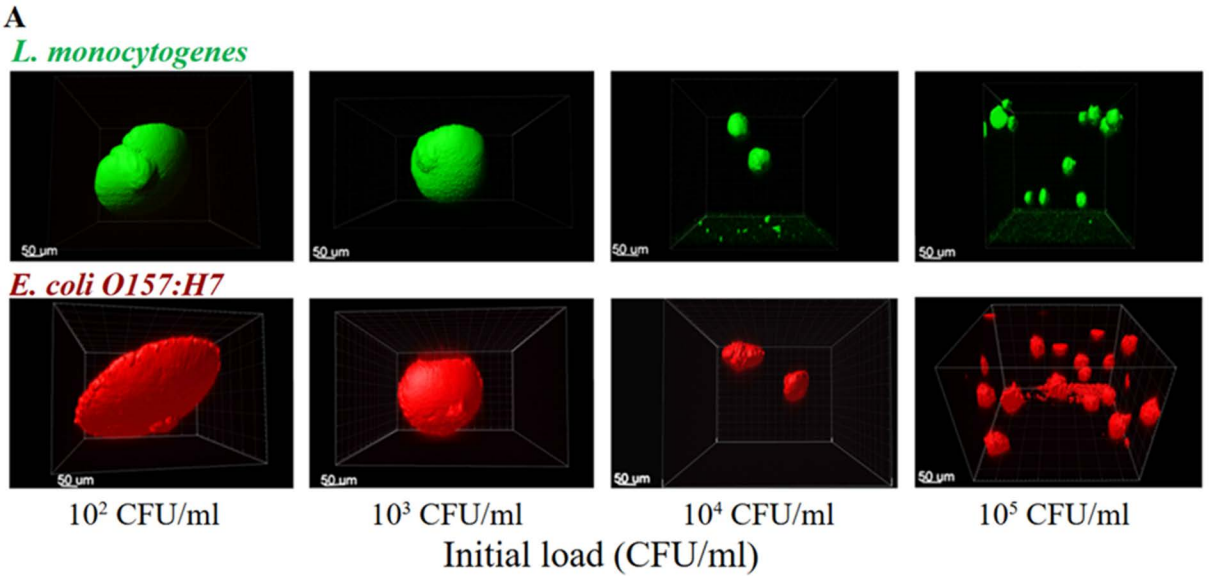
A
L. monocytogenes
E. coli O157:H7
50 µm
10² CFU/ml
10³ CFU/ml
10⁴ CFU/ml
10⁵ CFU/ml
Initial load (CFU/ml)

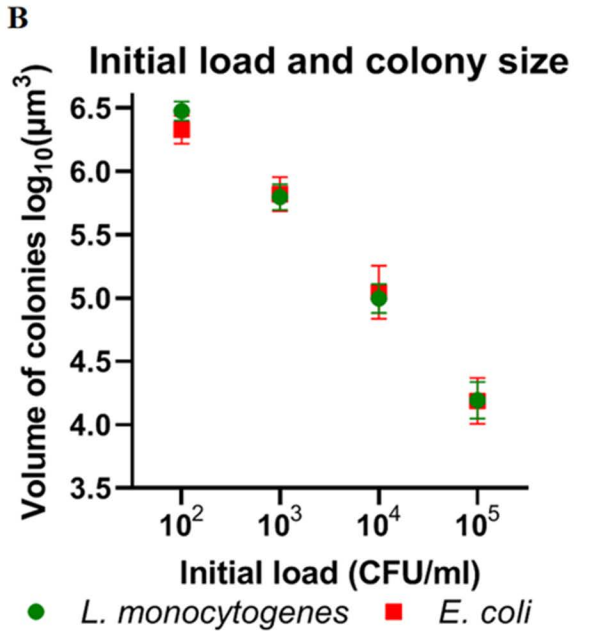
B
Initial load and colony size
Volume of colonies log10(µm3)
6.5
6.0
5.5
5.0
4.5
4.0
3.5
10²
10³
10⁴
10⁵
Initial load (CFU/ml)
L. monocytogenes
E. coli

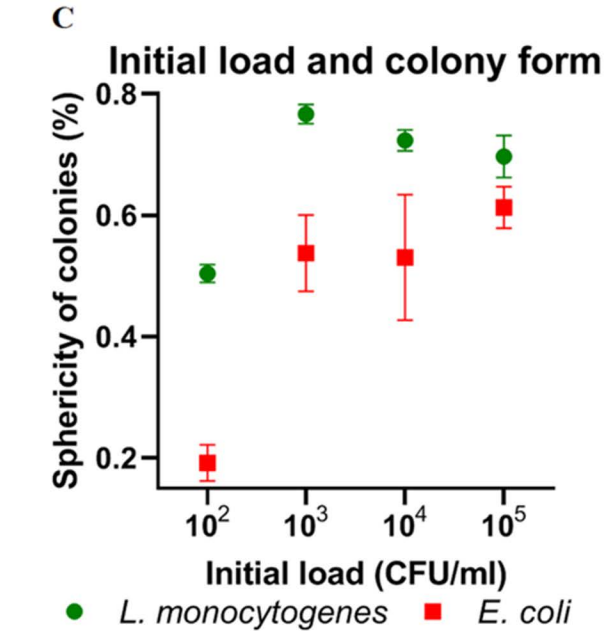
C
Initial load and colony form
Sphericity of colonies (%)
0.8
0.6
0.4
0.2
10²
10³
10⁴
10⁵
Initial load (CFU/ml)
L. monocytogenes
E. coli

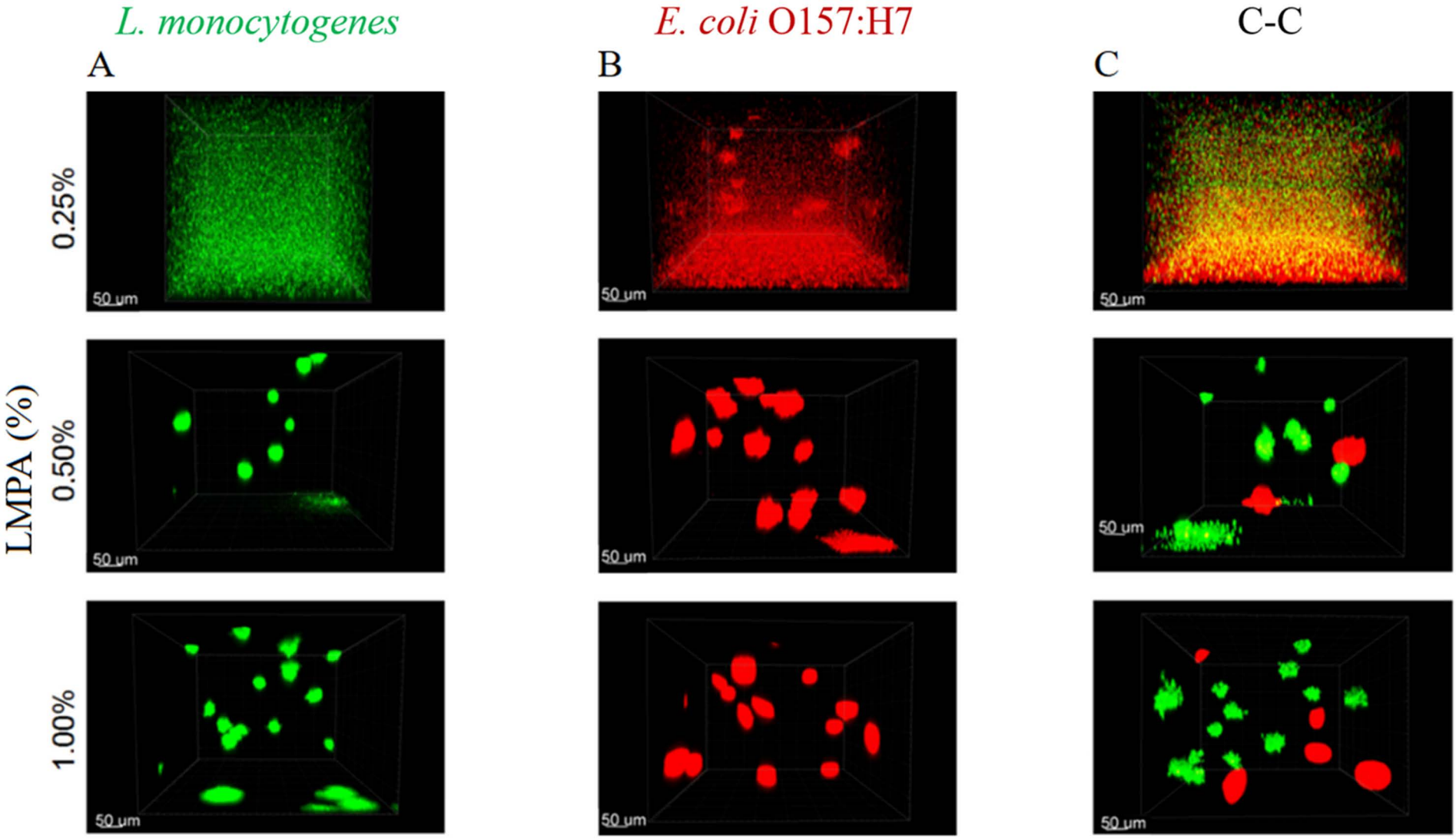
L. monocytogenes
E. coli O157:H7
C-C
A
B
C
LMPA (%)
0.25%
0.50%
1.00%
50 µm

A

Control | Lactic acid | NaCl | Lactic acid & NaCl

L. monocytogenes LMPA (%): 0.25% | 0.50% | 1.00%

E. coli O157:H7 LMPA (%): 0.25% | 0.50% | 1.00%

C-C LMPA (%): 0.25% | 0.50% | 1.00%

50 µm

B

LMPA (%)

L. monocytogenes | *E. coli* O157:H7

Control: 0.25% | 0.50% | 1.00%

Lactic acid: 0.25% | 0.50% | 1.00%

NaCl: 0.25% | 0.50% | 1.00%

Lactic acid & NaCl: 0.25% | 0.50% | 1.00%

M-C 48h | M-C 96h | C-C 48h | C-C 96h | M-C 48h | M-C 96h | C-C 48h | C-C 96h

Log_{10} scale of the biovolume of microcolonies (μm^3)

Microcolonies

Single cells and aggregates

4 | 3 | 2 | 1

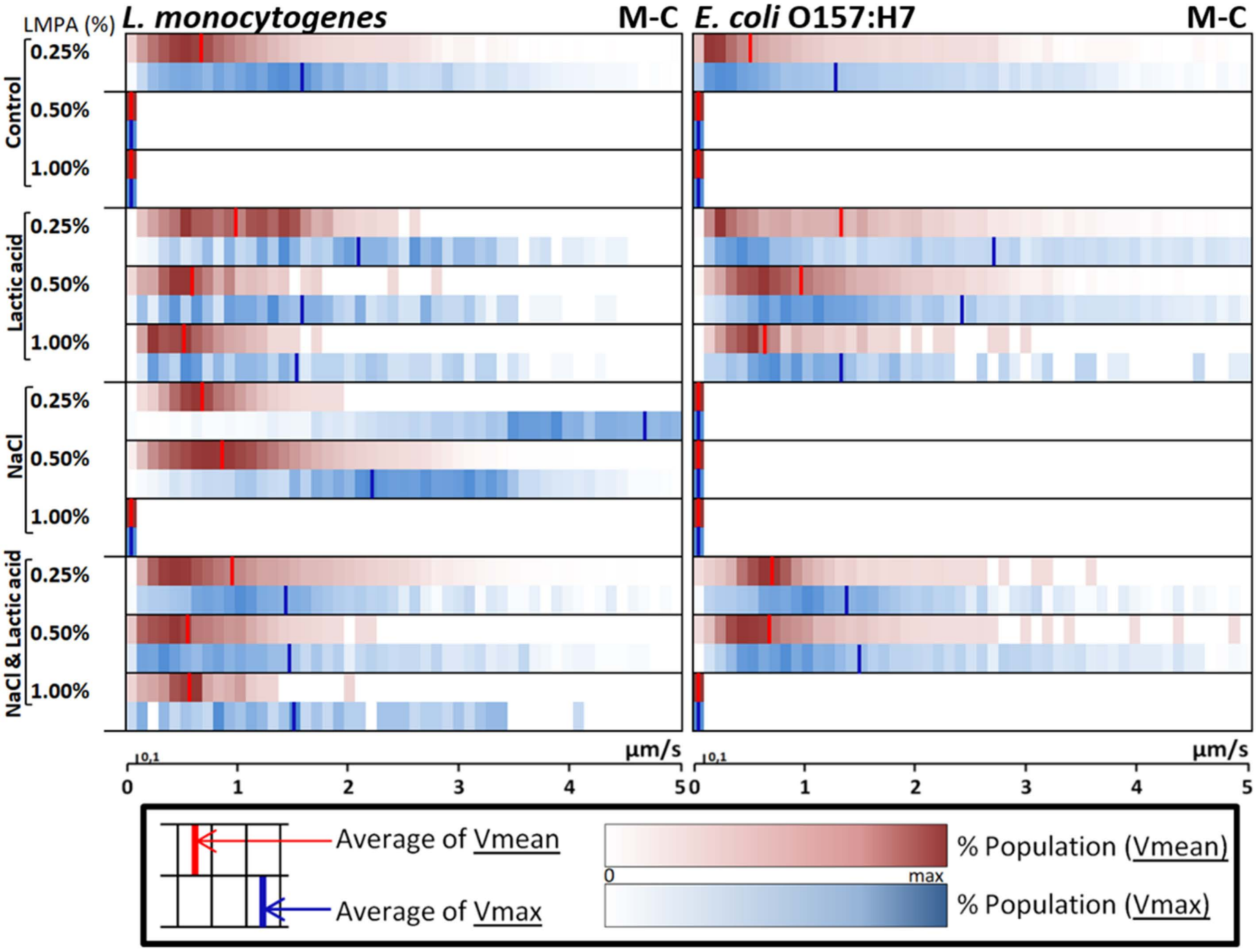
LMPA (%)
L. monocytogenes
M-C
E. coli O157:H7
M-C
Control
Lactic acid
NaCl
NaCl & Lactic acid
0.25%
0.50%
1.00%
µm/s
0,1
0
1
2
3
4
5
Average of Vmean
Average of Vmax
% Population (Vmean)
% Population (Vmax)
0
max

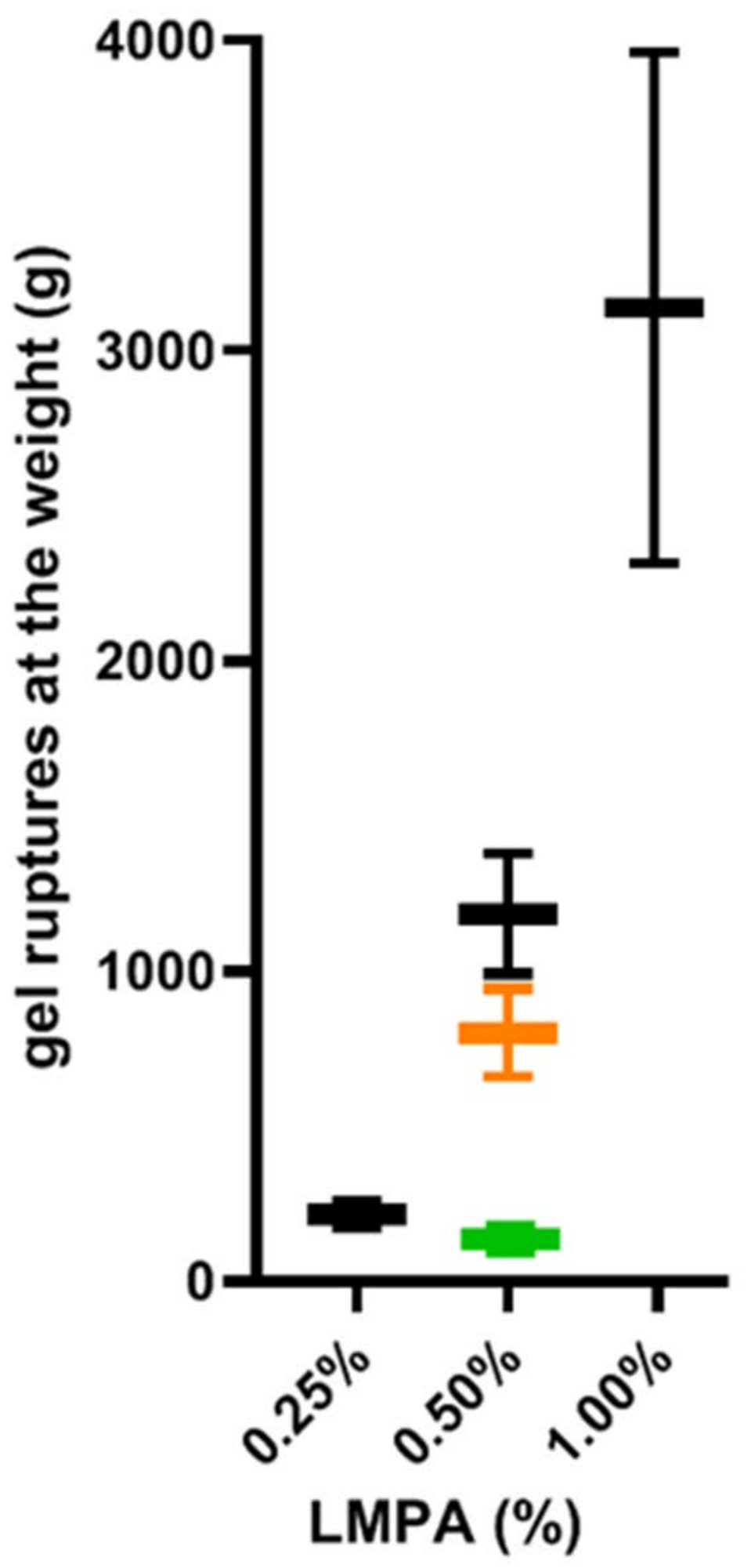
4000
3000
2000
1000
0
gel ruptures at the weight (g)
0.25%
0.50%
1.00%
LMPA (%)

L. monocytogenes

E. coli O157:H7

A

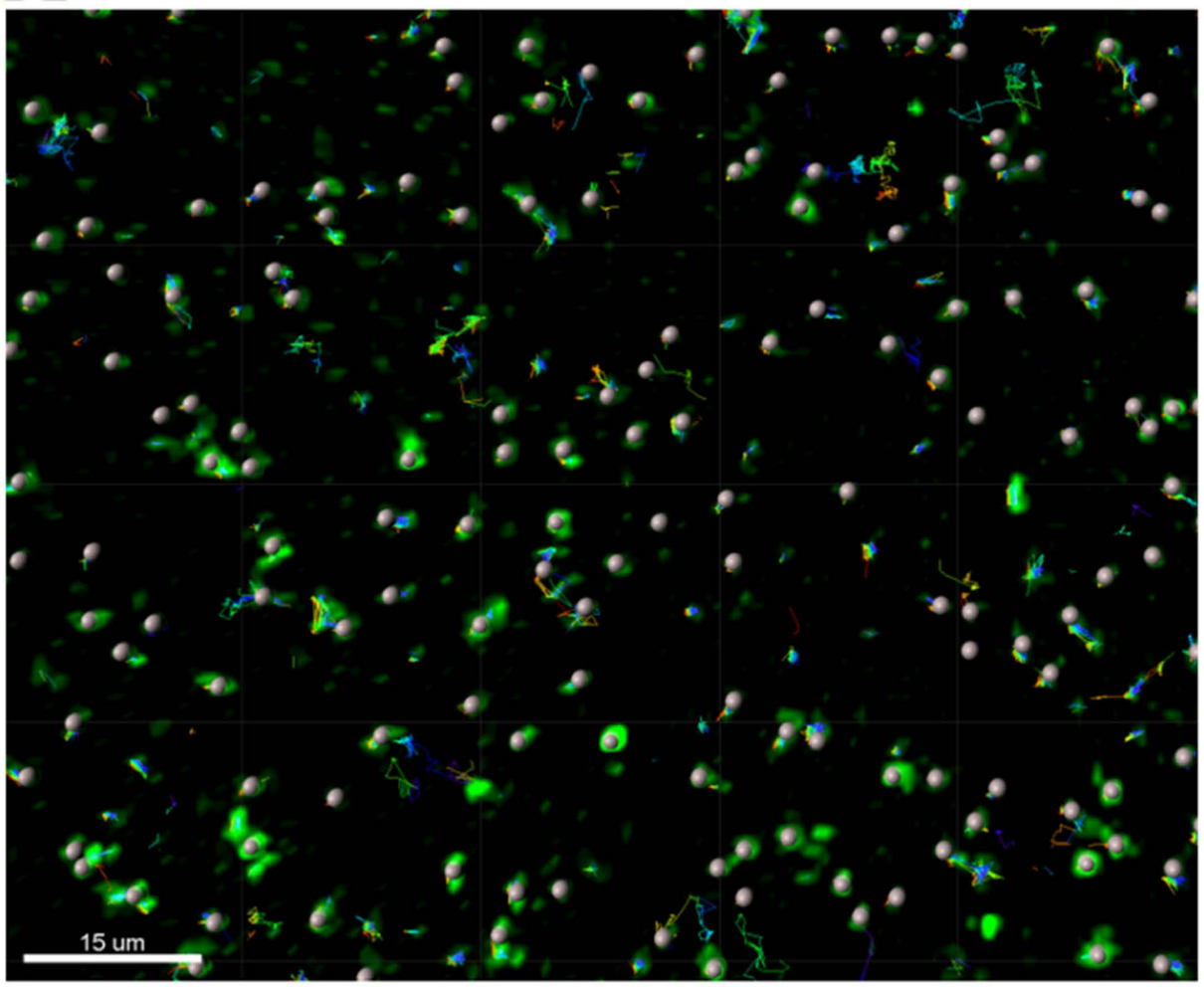

D

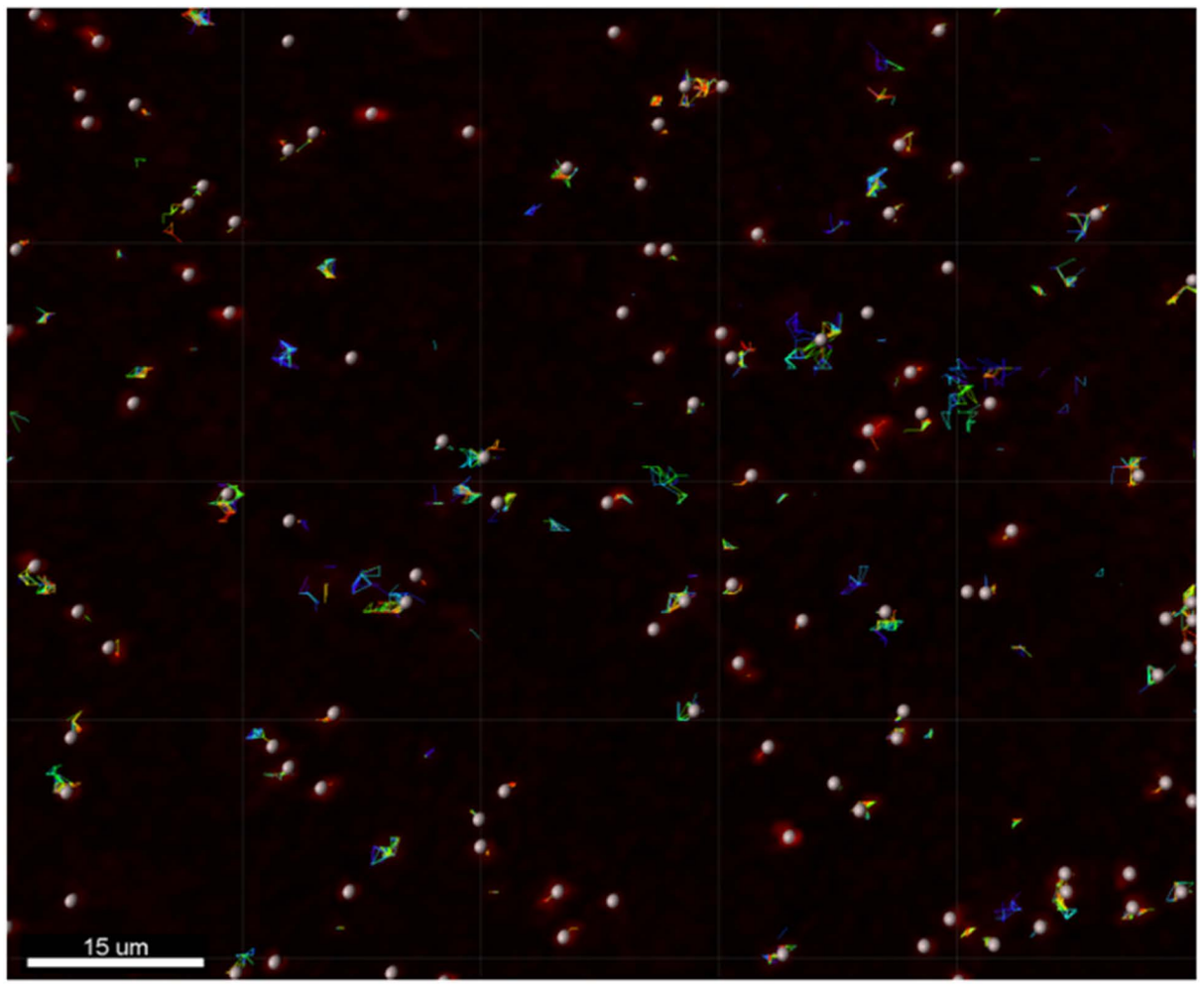

0.25% LMPA, Control

B

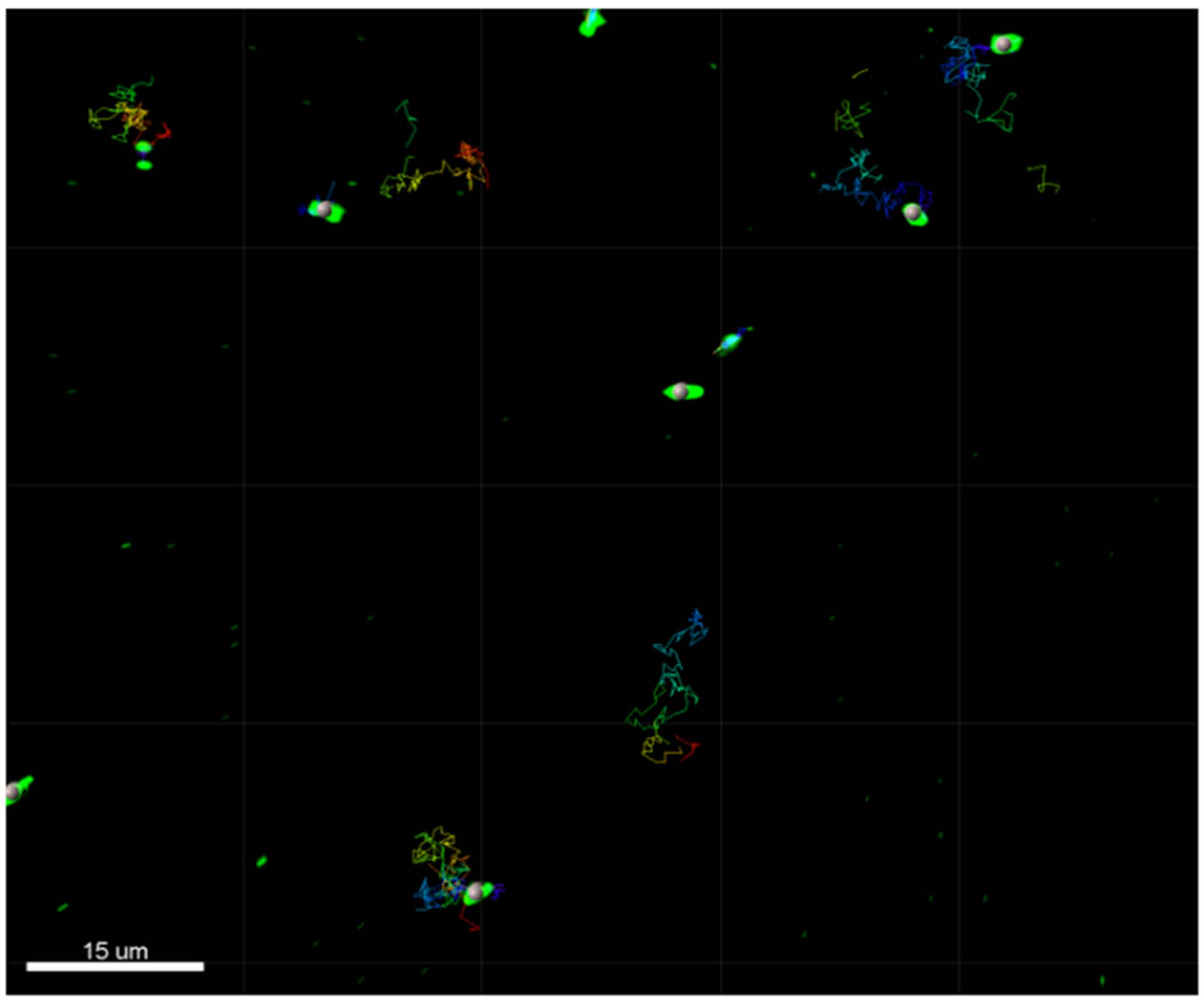

E

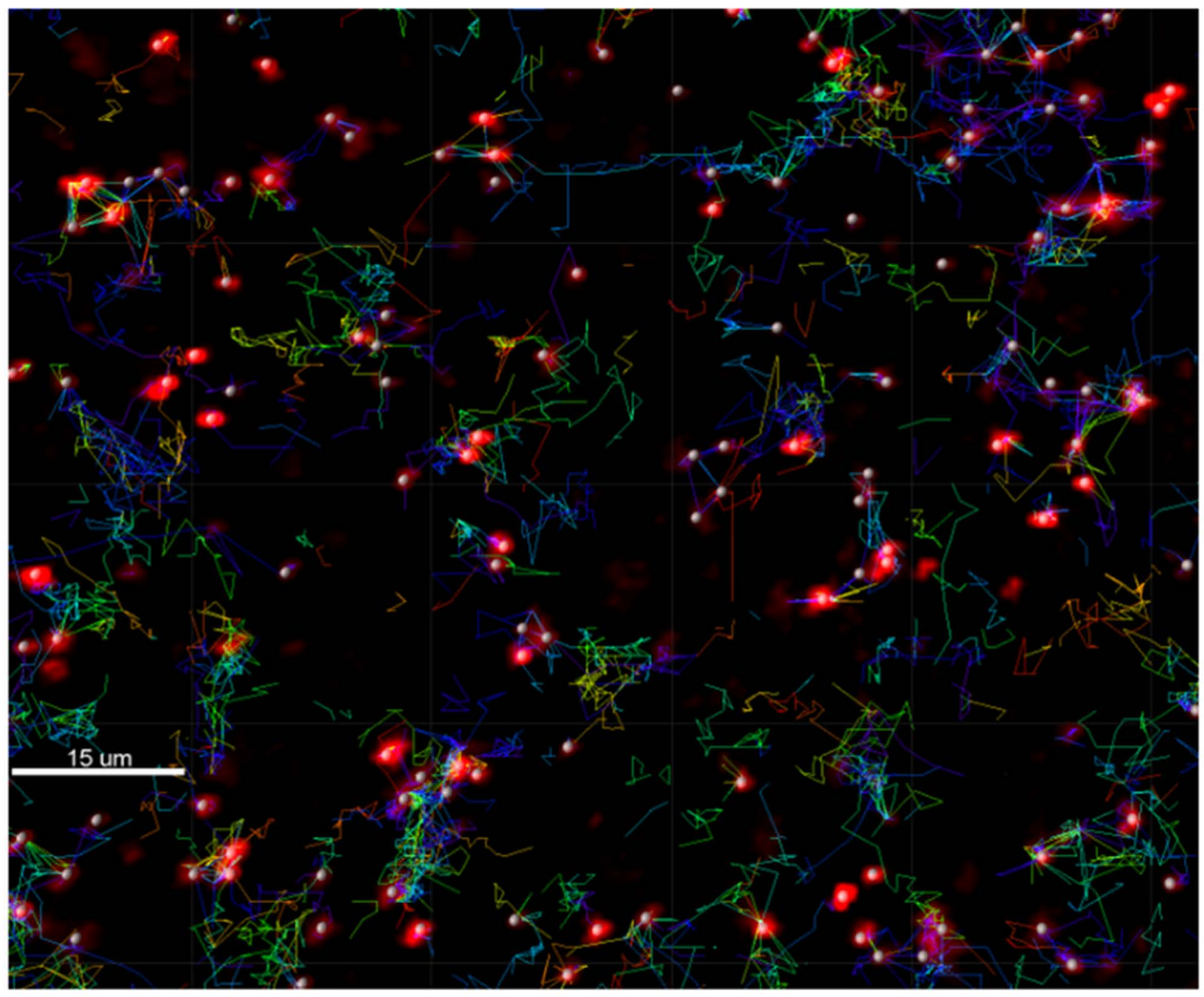

0.25% LMPA, Lactic acid

C

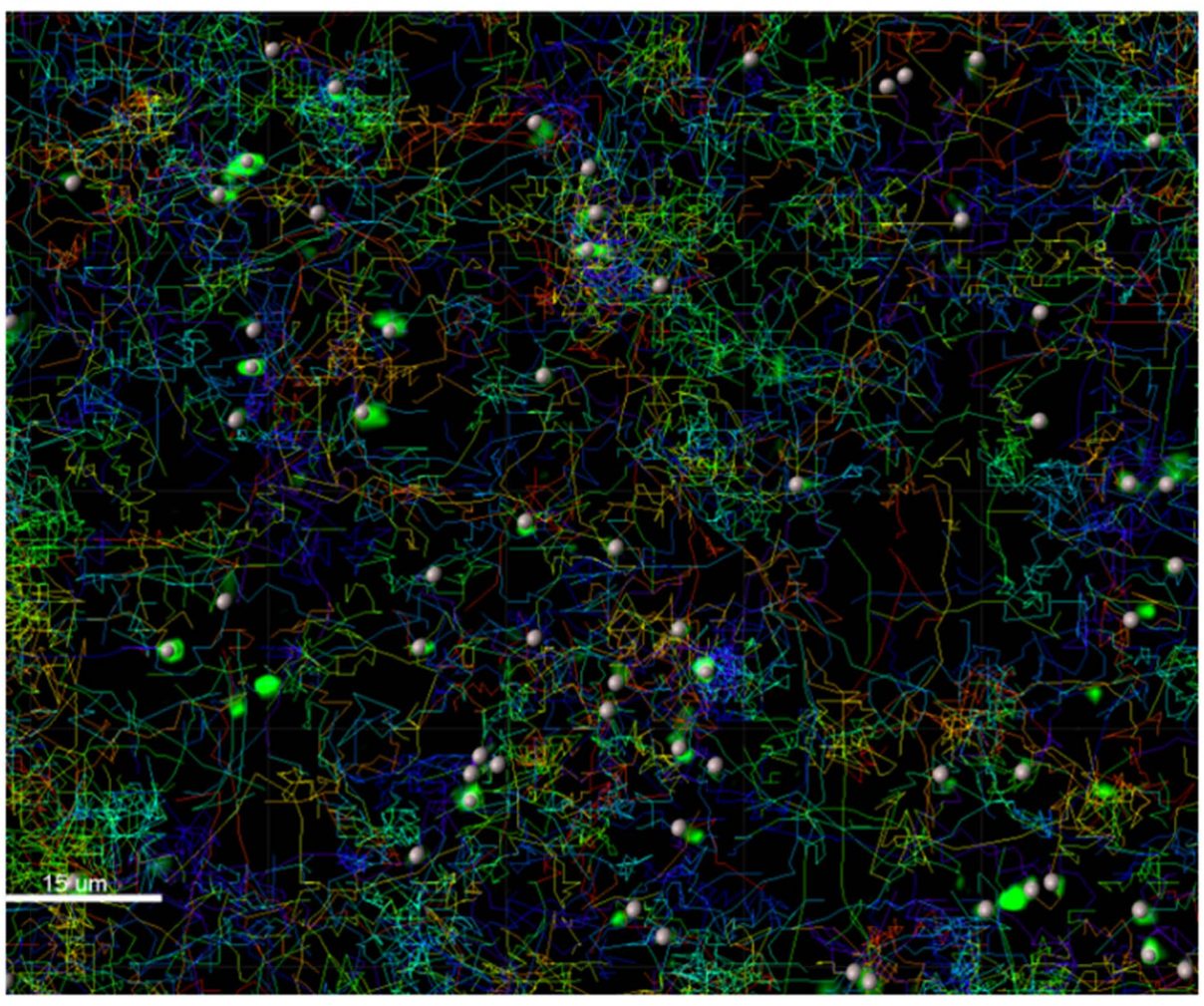

F

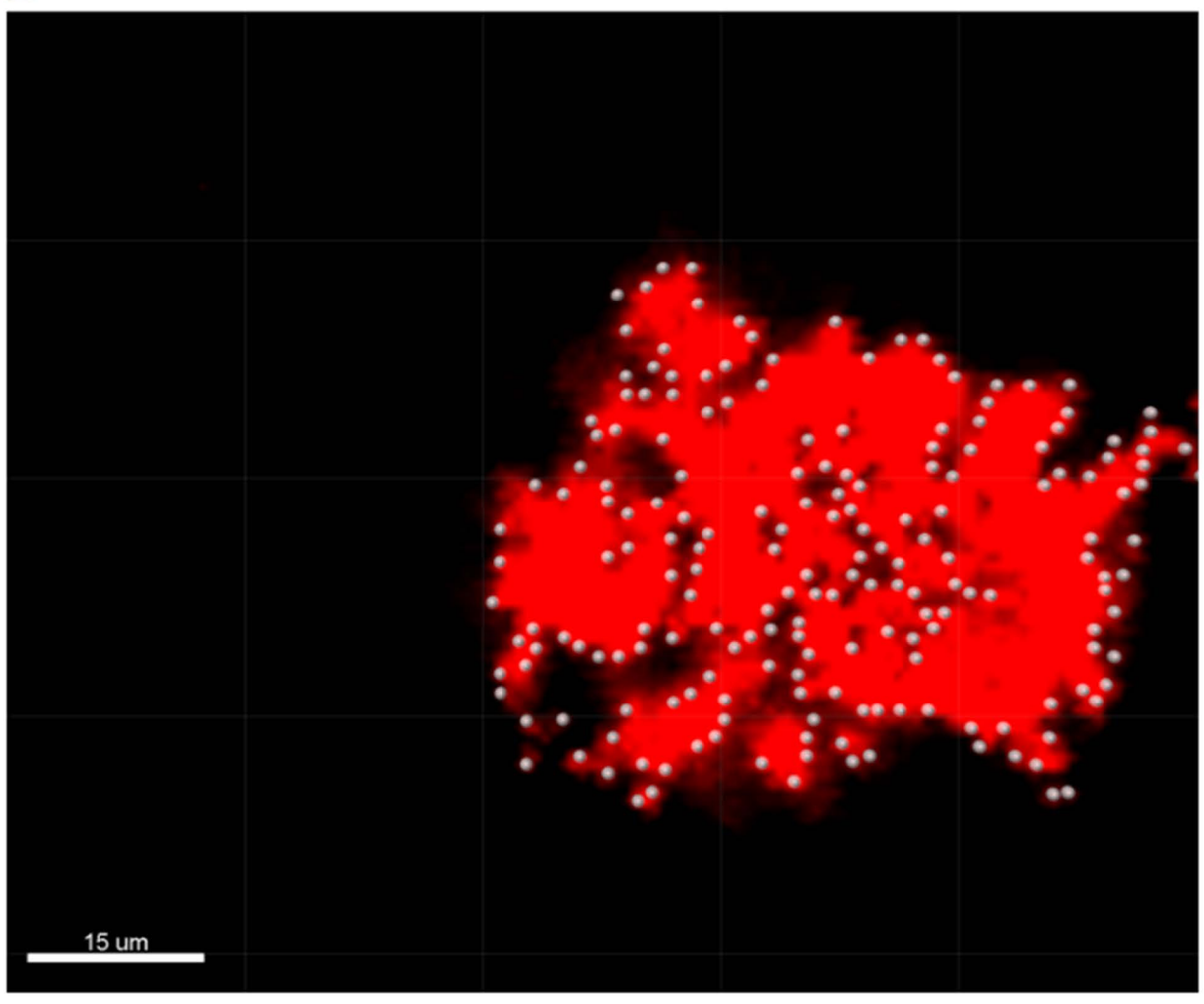

0.25% LMPA, NaCl

Supplementary material

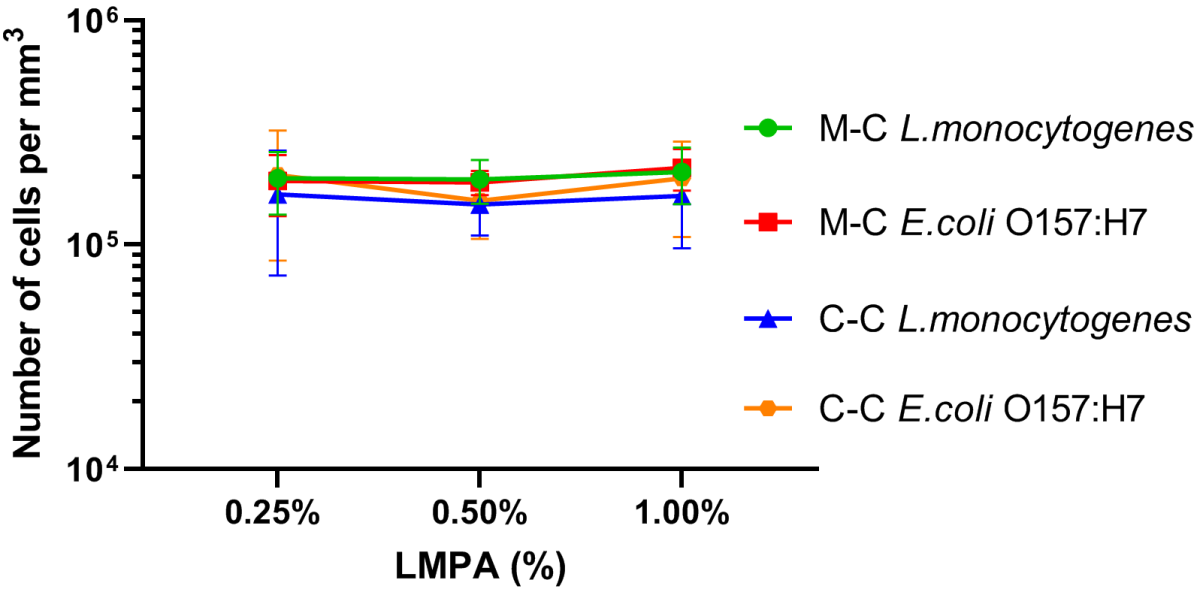

Figure S1: Quantitative analysis of the cell population per image (Material and Method) of *L. monocytogenes* and *E. coli* O157:H7 in mono- and co-cultures between three values of LMPA concentration Media are inoculated at 10^2 CFU/ml and cultivated at 20°C for 96 h.

Log(CFU/ml)	**TSB**	**TSB 0.25 LMPA**	**TSB pH5**	**TSB pH5 0.25% LMPA**	**TSB NaCl**	**TSB NaCl 0.25% LMPA**
L. monocytogenes	9.36±0.19	9.48±0.13	9.00±0.43	4.87±0.25	9.39±0.20	8.02±0.31
***E. coli* O157:H7**	9.25±0.11	9.30±0.10	9.00±0.29	7.00±0.24	9.08±0.18	8.62±0.19

Figure S2: Table of final CFU/ml achieved in either TSB or 0.50 % LMPA in conditions: control, lactic acid, NaCl. Media are inoculated at 10^2 CFU/ml and cultivated at 20°C for 96 h. Supplementation by lactic acid or NaCl is as described in the Materials and Methods.

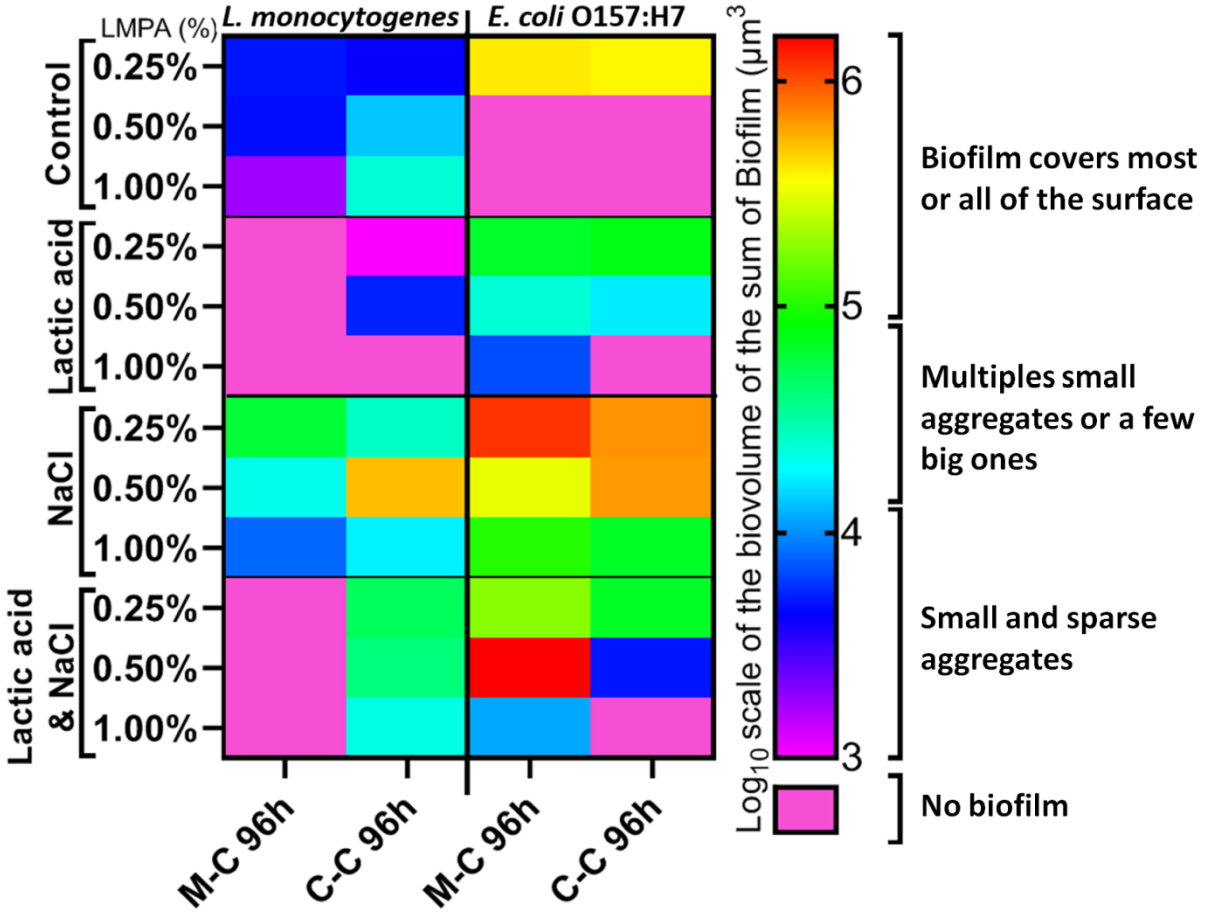

Figure S3: Impact of lactic acid and/or NaCl supplementation on biofilm of *L. monocytogenes* and *E. coli* O157:H7 in gelled matrices. Heatmap of the mean biovolume of biofilms in the different gelled matrix conditions. The colour scale is expressed in $\log_{10}$ (μm^3) with cooler tones indicating smaller amounts of biofilm and warmer colours are attributed to bigger amounts of biofilm. Data originate from CLSM observations performed at 96 h from mono-culture (M-C) and co-culture (C-C) conditions.

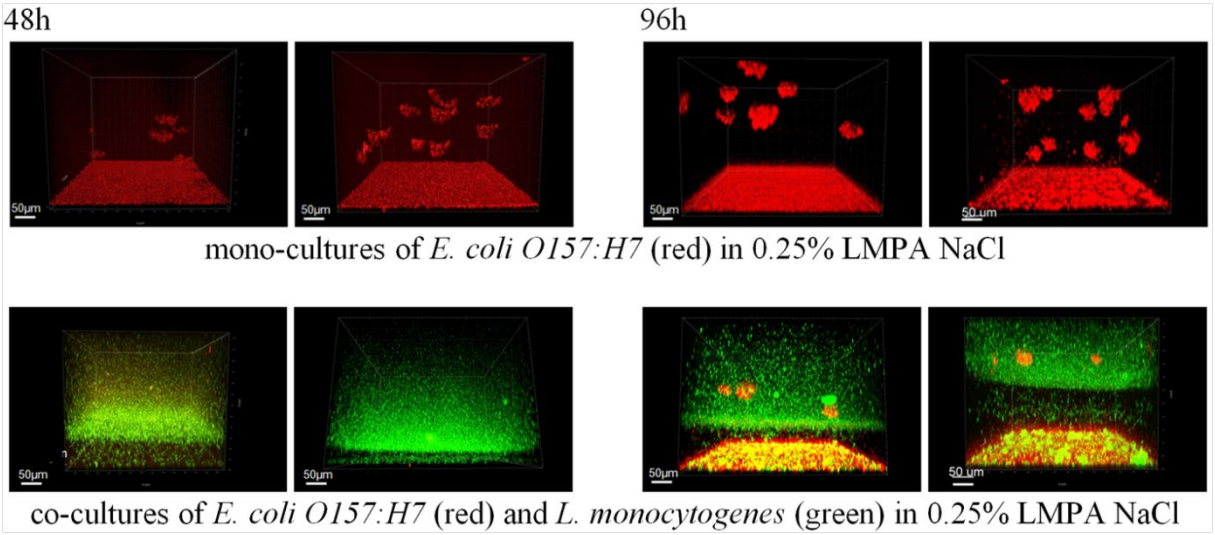

Figure S4: Qualitative observation of the growth delay for microcolonies of *E. coli* O157:H7 caused by the presence of *L. monocytogenes.* Gelled matrices were obtained at 0.25 % LMPA and supplemented with NaCl. For mono-cultures of *E. coli* O157:H7, four observations are shown, two at 48 h (left side) and two at 96 h (right side). The same was done with co-cultures of *L. monocytogenes* and *E. coli* O157:H7.

Conditions:	VMean µm/s	Standard deviation Vmean	Vmax µm/s	Standard deviation Vmax
***L. monocytogenes* mono-cultures**				
0.25% LMPA control	0.68	0.42	1.57	1.11
0.50% LMPA control	0.00	0.00	0.00	0.00
1.00% LMPA control	0.00	0.00	0.00	0.00
0.25% LMPA lactic acid	0.99	0.47	2.07	1.01
0.50% LMPA lactic acid	0.61	0.38	1.59	0.98
1.00% LMPA lactic acid	0.54	0.30	1.55	1.02
0.25% LMPA NaCl	0.68	0.26	4.77	1.92
0.50% LMPA NaCl	0.95	0.53	2.22	1.16
1.00% LMPA NaCl	0.00	0.00	0.00	0.00
0.25% LMPA lactic acid & NaCl	0.96	0.71	1.39	1.05
0.50% LMPA lactic acid & NaCl	0.57	0.37	1.47	1.10
1.00% LMPA lactic acid & NaCl	0.58	0.30	1.56	1.02
***E. coli* O157:H7 mono-cultures**				
0.25% LMPA control	0.53	0.54	1.27	1.34
0.50% LMPA control	0.00	0.00	0.00	0.00
1.00% LMPA control	0.00	0.00	0.00	0.00
0.25% LMPA lactic acid	1.36	1.04	2.70	1.84
0.50% LMPA lactic acid	0.97	0.64	2.41	1.73
1.00% LMPA lactic acid	0.67	0.48	1.36	1.06
0.25% LMPA NaCl	0.00	0.00	0.00	0.00
0.50% LMPA NaCl	0.00	0.00	0.00	0.00
1.00% LMPA NaCl	0.00	0.00	0.00	0.00
0.25% LMPA lactic acid & NaCl	0.72	0.39	1.39	1.05
0.50% LMPA lactic acid & NaCl	0.70	0.48	1.58	1.16
1.00% LMPA lactic acid & NaCl	0.00	0.00	0.00	0.00

Figure S5: Table of average Vmean and Vmax speeds values and standard deviations for each condition of mono-cultures (see Figure 4). Each value is calculated from a few hundreds to a thousand measures.

33 **A**

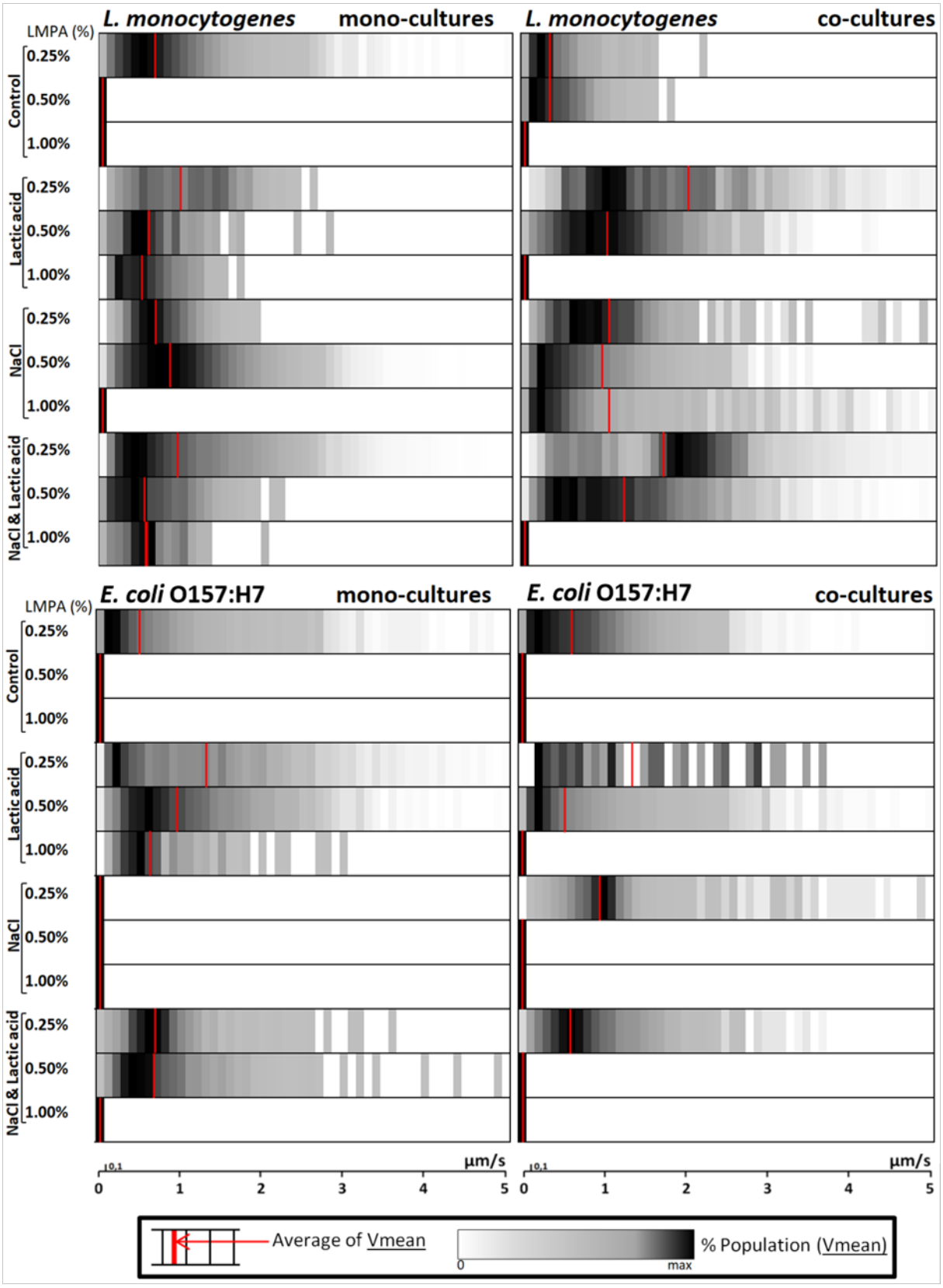
L. monocytogenes mono-cultures
L. monocytogenes co-cultures
E. coli O157:H7 mono-cultures
E. coli O157:H7 co-cultures
LMPA (%)
Control
Lactic acid
NaCl
NaCl & Lactic acid
0.25%
0.50%
1.00%
0
1
2
3
4
5
µm/s
Average of Vmean
% Population (Vmean)
max

34

35

B

Conditions:	Vmean µm/s	Standard deviation Vmean
***L. monocytogenes* co-cultures**		
0.25% LMPA control	0.35	0.29
0.50% LMPA control	0.37	0.26
1.00% LMPA control	0.00	0.00
0.25% LMPA lactic acid	2.08	1.33
0.50% LMPA lactic acid	1.07	0.58
1.00% LMPA lactic acid	0.00	0.00
0.25% LMPA NaCl	1.09	1.03
0.50% LMPA NaCl	0.92	0.43
1.00% LMPA NaCl	1.08	1.52
0.25% LMPA lactic acid & NaCl	1.74	0.85
0.50% LMPA lactic acid & NaCl	1.28	0.84
1.00% LMPA lactic acid & NaCl	0.00	0.00
***E. coli* O157:H7 co-cultures**		
0.25% LMPA control	0.66	0.49
0.50% LMPA control	0.00	0.00
1.00% LMPA control	0.00	0.00
0.25% LMPA lactic acid	1.38	1.01
0.50% LMPA lactic acid	0.57	0.54
1.00% LMPA lactic acid	0.00	0.00
0.25% LMPA NaCl	1.00	0.56
0.50% LMPA NaCl	0.00	0.00
1.00% LMPA NaCl	0.00	0.00
0.25% LMPA lactic acid & NaCl	0.79	0.46
0.50% LMPA lactic acid & NaCl	0.00	0.00
1.00% LMPA lactic acid & NaCl	0.00	0.00

Figure S6: Analysis of cell motility of *L. monocytogenes* and *E. coli* O157:H7 in different gelled matrix conditions for mono- and co-cultures (A). The mean speed (Vmean) was calculated from bacterial cell observations in time-lapse microscopy as described in the Material and Methods section. From there, the percentage of population for the different speed values was represented as a density bar. The averages for the Vmean were further calculated and represented as bright colour lines (red) to highlight shift in motility of the cell population. Gelled matrices were obtained at different LMPA (i.e. 0.25 %, 0.50 % or 1.00 %) concentrations (i) without the addition of lactic acid or NaCl (control condition), (ii) with the addition of lactic acid (pH 5), (iii) with supplementation of NaCl, or (iv) with both lactic acid and NaCl. **(B).** Table recapitulating the average Vmean values and standard deviations for each condition of mono- and co-cultures Each value is calculated from a few hundreds to a thousand measures.

Supplementary movies: All timelapse were realised on cultures after 96 h at 20°C. Timelapses have a 2 minutes length with a frequency of 0.44s for a total of 275 images. Video were generated with Imaris software at 24frames/s and are 183 µm by 122 µm in size. Dragon-tails show 5 seconds of tracking. A tile image from each video with the full tracking is presented below. A close up of those same image are used in figure 6 of the article.

Video7A: *L. monocytogenes* in 0.25 % LMPA control

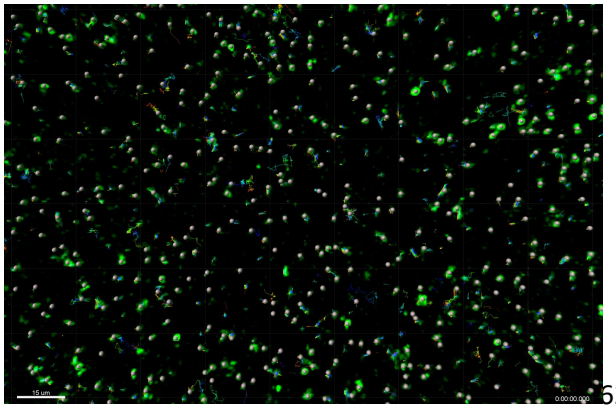

Video7B: *L. monocytogenes* in 0.25 % LMPA lactic acid

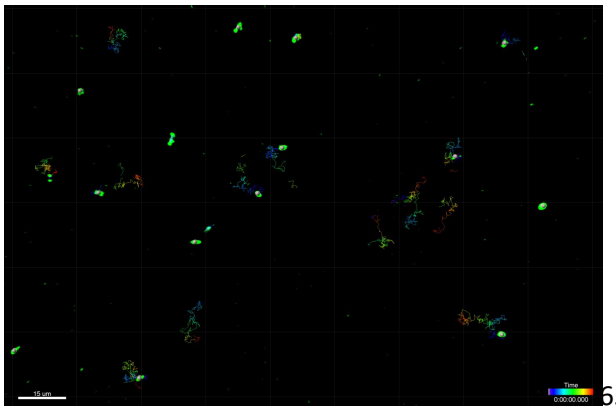

Video7C: *L. monocytogenes* in 0.25 % LMPA NaCl

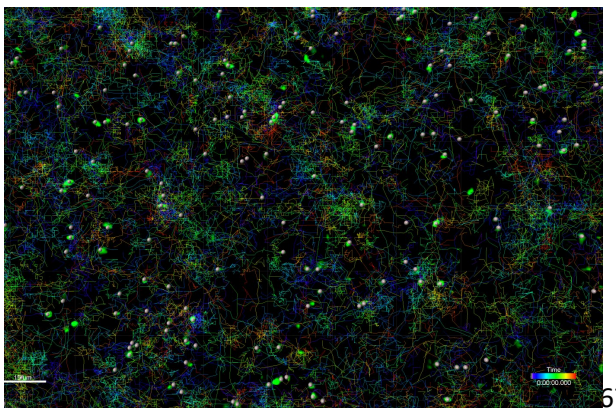

Video7D: *E. coli* O157:H7 in 0.25 % LMPA control

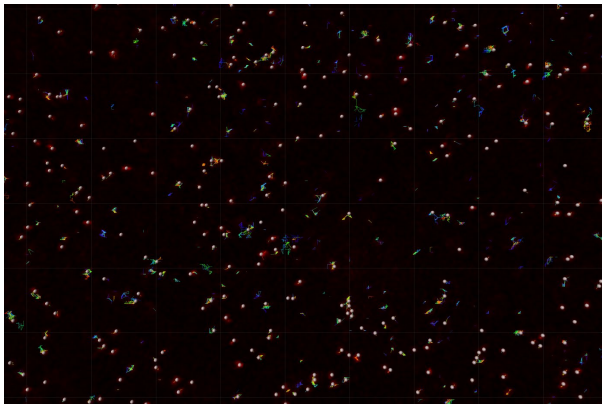

Video7E: *E. coli* O157:H7 in 0.25 % LMPA lactic acid

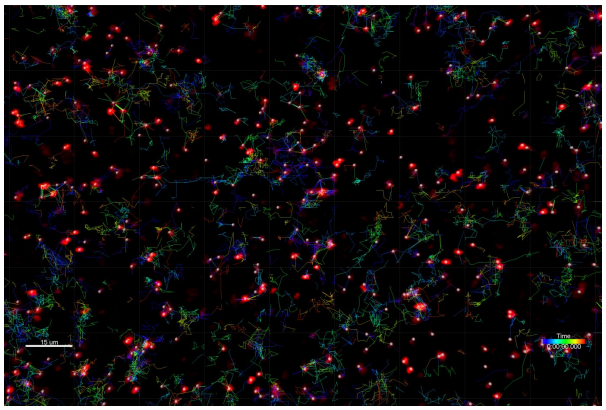

Video7F: *E. coli* O157:H7 in 0.25 % LMPA NaCl